Topics in Catalysis
https://doi.org/10.1007/s11244-024-01913-z

REVIEW PAPER

Catalysts for Clean Energy: A Review on Current Progress for the Catalyzed Recycling of CO_2 into Dimethyl Ether

Alexander Livescu[1] · Ricardo Navar[1] · Jasan Robey Mangalindan[2] · Fatima Mahnaz[2] · Yulu Ge[1] · Manish Shetty[2] · Xiaokun Yang[1]

Accepted: 17 January 2024

Abstract

Dimethyl ether (DME), one of the proposed targets for CO_2 recycling, is a very attractive renewable energy source due to its non-toxic nature, low environmental impact, and hydrogen (H_2)-carrying abilities. The thermal catalyzed reaction of CO_2 to DME requires two steps with different catalysts, and the combination and optimization of these catalysts are of great importance for achieving viable DME yield that would make future industrial implementation possible. The thermodynamics and reaction mechanisms of the CO_2 conversion to DME were discussed. The metallic and acidic catalyst functions utilized for this reaction are analyzed in this review, and the different methods of combination are presented with a focus on hybrid catalysts to achieve successful and efficient catalyzed reactions with optimized DME yield. Additionally, an outlook for future directions in catalyst development and mechanistic understanding in this largely overlooked area are provided.

Keywords Carbon dioxide · Dimethyl ether · Renewable fuel · Catalysis

1 Introduction

In the present day and age, energy is an indispensable part of our lifestyles. Our daily need for different types of energy (e.g., electricity, fuel, etc.) requires abundant energy sources, and according to the Environmental and Energy Study Institute (EESI), around 80% of our energy needs are powered by fossil fuels [1]. Unfortunately, our heavy dependence on fossil fuels results in large volumes of greenhouse gas emissions which are detrimental to the environment causing [2]. CO_2 is the most abundant greenhouse gas released into the atmosphere (Fig. 1). It is reported that 37 Gt had been released into the atmosphere in the year 2022 alone. From all the CO_2 generated by human activity, 42% of these emissions stem from power generation, 26% from transportation, 23% from manufacturing/construction, and 9% from other sources (e.g., residential) indicating the correlation between our energy-use and the release of CO_2 into our atmosphere [3]. Lot of efforts has been undertaken to address the reduction of CO_2 emissions and concentrations in the atmosphere. One of the most commonly implemented strategies to achieve this goal in the past was to use carbon capture and storage (CCS), a method of capturing CO_2 and storing it underground for long periods [4]. However, this process requires infrastructure and large amounts of capital to be put in use. Therefore, there is a strong desire to identify a suitable, uncomplicated, and cost-effective solution to address the challenge of climate change by mitigating CO_2 emissions, thereby fulfilling the significant demand for energy.

Increasing attention has been drawn to carbon dioxide utilization (CDU), as this method helps close the carbon cycle and creates a more sustainable approach to the creation and utilization of CO_2 [3, 5]. The interest in CDU dates back to the 1970s, and it has increasingly gained momentum as the demand for a solution to the issue of greenhouse gases has grown. The CDU process involves the capture of CO_2 to for recycling into both value-added products and fuels. In parallel with CDU, CO_2 can be used directly in commercial products and services such as oil recovery, beverage carbonation, food processing, and solvents [4]. However, these

Alexander Livescu and Ricardo Navar are the first authors.

✉ Xiaokun Yang
xiaokuny@lanl.gov

1 Chemistry Division at Los Alamos National Laboratory, Los Alamos, NM, USA

2 Artie McFerrin Department of Chemical Engineering, Texas A&M University, 100 Spence Street, College Station, TX 77843, USA

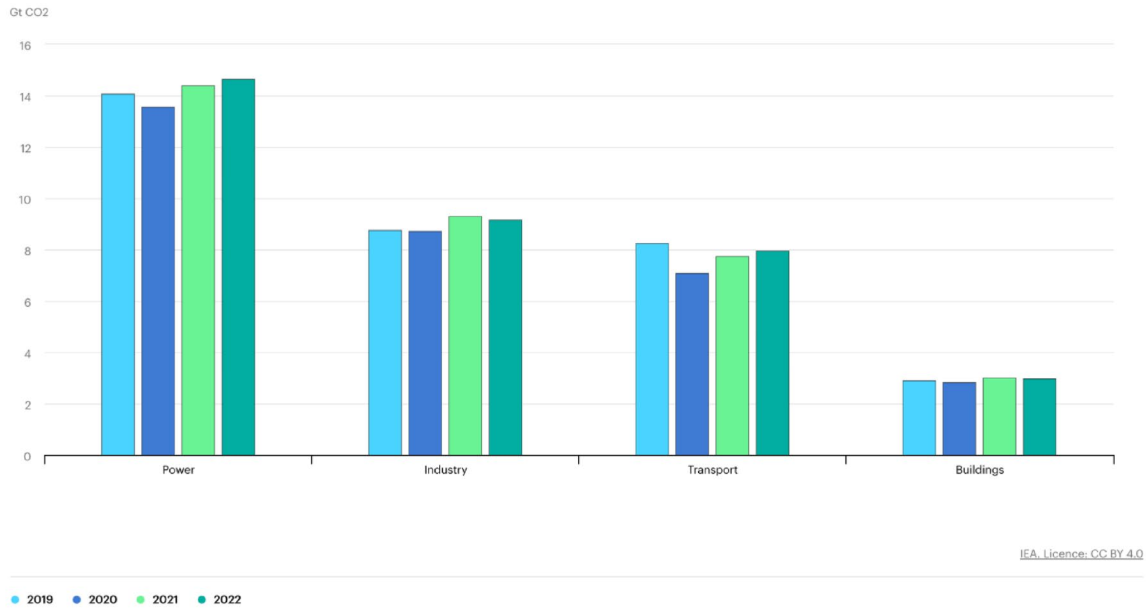

Fig. 1 CO_2 emissions by sector from 2019 to 2022

direct applications would only account for a small percentage of the available CO_2. Consequently, there is a stronger focus on utilizing CO_2 as a chemical feedstock, as this can have a much larger impact on CO_2 levels in our environment. Every year, around 110 million metric tons of CO_2 are used as a raw material for the production of urea, methanol, polycarbonates, cyclic carbonates and specialty chemicals.

Over the past two decades, numerous technologies and advanced mythologies have emerged to reduce CO_2 emission and enhance utilization. Examples include photochemical reduction, thermochemical reduction, chemical reduction, electrocatalytic reduction, radiochemical methods, biochemically reduction, enzymatic electrosynthesis, and more. These diverse approaches yield multiple products depending on the catalysts used sand the reaction's selectivity, such as CH_4, CO, HCOOH, C_2H_6, HCHO, CH_3CH_2OH, C_2H_4, and CH_3OH. Here is this review, we will focus on thermal catalytic pathway which is a promising approach to utilize current existing industrial equipment, facilities, and infrastructure. One of the largest thermal catalytic pathways through for the utilization of CO_2 is its conversion to methanol due to its high demand (57 Mt per year) [6]. Lots of studies has been focus on one-step conversion from CO_2 to methanol conversion [3, 7, 8]. Additionally, methanol can then be converted to produce many value-added products and renewable fuels. Among these CO_2 derived products, dimethyl ether (DME) has recently garnered significant research interest. Our group has studied the DME as an alternative renewable fuel from thermodynamics, fuel properties and economic feasibilities perspectives [9]. In this review, we will highlight the advantages and challenges of DME synthesis by using one of the renewable carbon sources, CO_2. Synthesis of DME via catalytical hydrogenation of CO_2 is a promising approach since it is thermodynamically favored over methanol. It could occur in two ways: (a) two-step synthesis wherein CO_2 is converted to methanol, which is subsequently converted to DME, or (b) a one-pot synthesis wherein CO_2 is directly converted to DME. In previous studies, this reaction pathway has been performed by placing catalysts for each step in separate chambers and flowing the reaction mixture stepwise through each chamber, forming a continuous reaction channel [10]. However, recent advances have shown that integrates these two steps by mixing the two catalysts is able to synthesis of DME directly from CO_2 with drastically improved the efficiency. As a result, increased the economic viability of its industrial implementation [11–13]. Both the two-step reaction system and the one-pot synthesis of DME will be covered in this review.

DME is a subject of interest due to its similar physical properties with liquefied petroleum gas (LPG) (i.e., propane and butane) and its potential use as a diesel fuel replacement [8, 9]. The technologies used for the storage and transportation of LPG may be used for DME without additional considerations [14]. In addition, DME's high cetane number (55–60) allows it to be easily blended with diesel making it feasible to apply in current diesel engines without the need for any modification. Although methanol is also being considered as an additive for gasoline engines due to its high octane number (Anti Knock Index of 98.65), it faces several issues such as high vapor pressure and separation in the presence of water which makes it difficult to be used in high concentrations in unmodified gasoline engines. Furthermore, DME possesses a higher net calorific value than methanol (31.7 vs. 22.9 MJ/kg HHV) resulting in a 30% higher energy output per volume than methanol [15]. Unlike the poisonous fact of methanol, DME is considered non-carcinogenic and non-toxic, contrary to methanol which is considered toxic, allowing for much safer implementation as well as cleaner use as a fuel (lowered pollutant output) [9, 16]. Its chemical composition without the presence of sulfur and nitrogen contributes to very low NO_x, SO_x and soot emissions, as well as reduced CO production, making it a heavily desired fuel substitute [6].

Like methanol, DME can also serve as a good hydrogen carrier. However, research on DME as a hydrogen carrier has been largely overlooked in the global community. DME boasts a higher hydrogen gravimetric capacity of 13 wt.% than methanol (12.5 wt.%) and a volumetric capacity of 87 kg H_2/m^3 albeit lower than methanol (99 kg H_2/m^3) [14]. DME steam reforming (DME-SR) to generate hydrogen is thermodynamically feasible, requiring reaction temperatures as low as 200 °C to achieve 99.9% conversion, as compared to 800 °C for traditional hydrocarbon fuels (natural gas, gasoline, diesel) or in a lower temperature but with precious metals. DME-SR produces comparable hydrogen contents but with no toxicity issues in materials handling as compared to methanol.

Strategies to produce DME from sequestered CO_2 offer a promising approach to developing carbon–neutral hydrogen carriers [14]. For example, combining direct air capture (DAC) and the CO_2 to DME catalytic process has the potential to offer a clean and carbon–neutral method for the removal of CO_2 from the atmosphere and producing clean fuel in return. DAC is a relatively new concept that involves the removal of CO_2 from ambient atmospheric air utilizing sorbents [17]. Although DAC is not currently at a stage of successful implementation, if further improvement brings it to this point, the process could provide a readily available feedstock of CO_2 that can be converted into fuels such as DME, presenting a possible method for large reductions in emissions in which the conversion of CO_2 to DME plays an important role.

Herein, this review summarizes the most recent and current work entailing CO_2 conversion to DME, focusing on the one-pot synthesis as the most efficient and promising reaction method of the topic. We first cover the favorable thermodynamics of the direct CO_2 hydrogenation to methanol, followed by its dehydration to DME. We overview reaction mechanism for DME formation along with the recent catalyst development for both synthesis methods. Additionally, we provide an outlook for future directions in catalyst development and mechanistic understanding in this largely overlooked area.

2 Reactions

The process of forming DME from CO_2 involves two individual reactions, the first forming methanol from CO_2 and the second turning the formed methanol into the desired product of DME. The initial CO_2 reacts with hydrogen gas as shown:

$$CO_2 + 3H_2 \rightarrow CH_3OH + H_2O \quad \Delta H^{\circ}_{298} = -41.4\,\text{kJ/mol}$$

The two methanol molecules formed in the above reaction react to form DME:

$$2CH_3OH \rightarrow CH_3OCH_3 + H_2O \quad \Delta H^{\circ}_{298} = -23.4\text{kJ/mol}$$

Thus, the overall reaction is:

$$2CO_2 + 6H_2 \rightarrow CH_3OCH_3 + 3H_2O \quad \Delta H^{\circ}_{298} = -106.2\text{kJ/mol}$$

It is also important to take the reverse water gas shift (RWGS) reaction into account:

$$CO_2 + H_2 \rightarrow CO + H_2O \quad \Delta H^{\circ}_{298} = 41.4\text{kJ/mol}$$

This process requires hydrogen gas, which is often produced through the consumption of fossil fuels. Even though, the hydrogen source is not our focus in this review, but it is inevitable to mention it because it is one of our major feed streams. We hold promise to a cleaner, more sustainable pathway to hydrogen gas production that will be implemented in order to make the process worthwhile to implement at a large, industrial scale. A number of solutions have been investigated (e.g., algae, biomass, etc.) and current clean hydrogen gas production often takes place through water electrolysis fueled by renewable electrical energy [18–20]. Water electrolysis to hydrogen gas is currently not at the highest efficiency (40–50%) but provides a very simple production system that is plausible to implement [21]. Although alkaline-based electrolysis is the most well-established, proton exchange membrane (PEM) and solid oxide electrolysis cell (SOEC) technologies are newly emerging, giving the process solid potential for further development [22]. Additionally, companies such as Oberon Fuels have begun to produce renewable DME from methanol at larger scales, proving the plausibility of this process.

As a matter of course, the thermodynamic favorability of each reaction must be considered as the combination of CO_2 to DME and RWGS presents limitations in DME production. A simple thermodynamic analysis of the one-pot synthesis of CO_2 to DME (Fig. 2) shows the effects of temperature and pressure on CO_2 conversion (X_{CO2}), DME selectivity (S_{DME}), methanol selectivity (S_{MeOH}), and CO selectivity (S_{CO}). The individual reactions of CO_2 to DME are both exothermic, and thus are favored at lower temperatures. However, increasing the temperature results in significant production of CO due to the endothermic nature of the RWGS reaction, which is problematic for various reasons: yield of DME will decrease as CO is thermodynamically favored at higher temperatures, and the

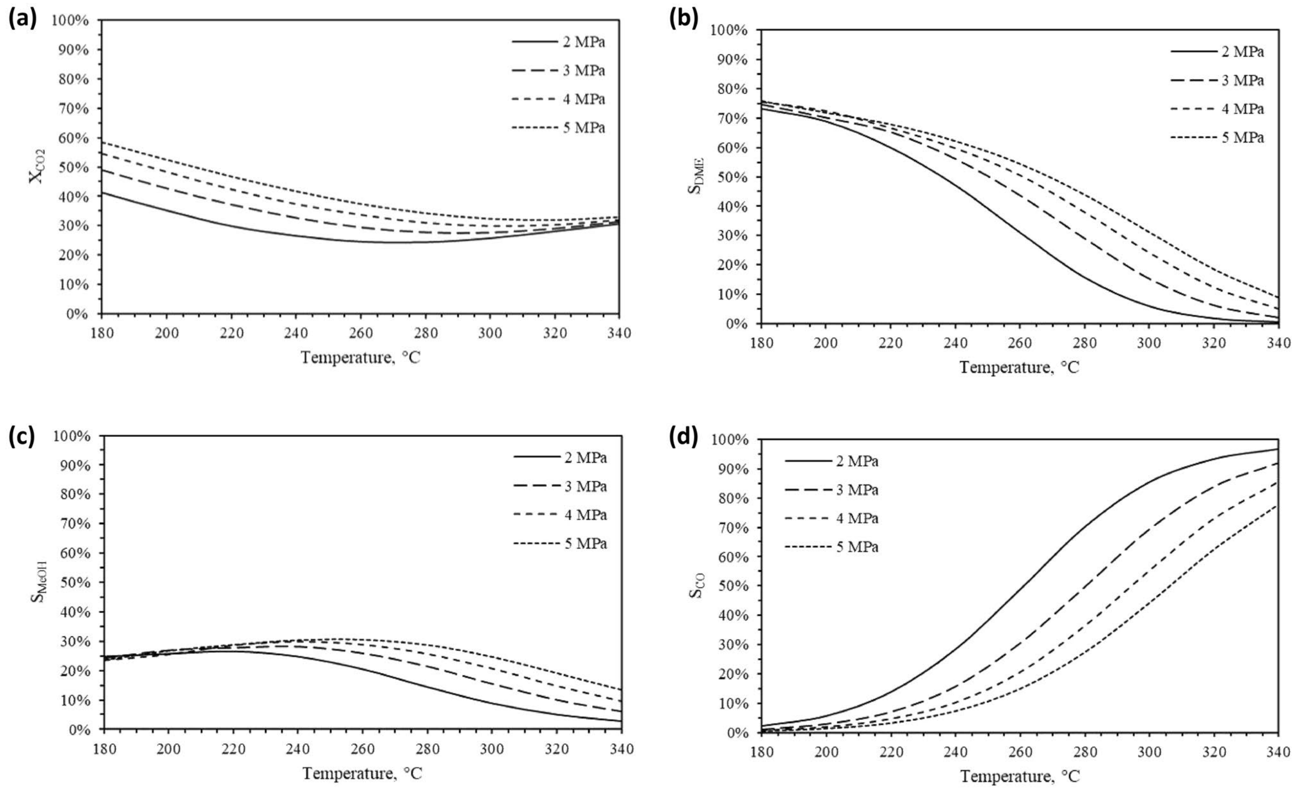

Fig. 2 Effect of temperature and pressure in **a** CO_2 conversion, **b** DME selectivity, **c** methanol selectivity, and **d** CO selectivity at equilibrium

produced CO must be consumed or disposed of carefully as it is considered a more dangerous and potent greenhouse gas than CO_2 [23]. Additionally, because of the low reactivity and relative stability of CO_2, a significant amount of energy is required to overcome its activation barrier in these reactions. Based on the stoichiometry of products and reactants in the overall reaction of CO_2 and DME, high pressures also favor the formation of DME, while the RWGS is unaffected, which ultimately improves selectivity to DME.

Therefore, reaction conditions must be carefully adjusted to maximize DME production despite the unintended consequence of the RWGS reaction. The exact temperature and pressure values vary depending on the reaction setup and the catalyst mixture used and must be experimentally determined. Temperatures are generally held between 200 and 300 °C and pressures are maintained between 2 and 5 MPa, although other values have been reported [24, 25], and we summarized them in Table 1.

As detailed, the large-scale implementation of DME production from CO_2 first requires some issues to be addressed, including the source of renewable hydrogen gas and limited production of unintended CO gas. However, the development of an efficient catalyst mixture can be incredibly influential to the hydrogen productivity and selectivity to help address the issues presented and accelerate large-scale industrial implementation, which would drastically affect our ability to combat CO_2 emissions.

3 Catalyst Overview

In order to optimize catalyst function and efficiency, it is important to understand the possible mechanisms of reaction utilized by each catalyst between different reactants. As demonstrated above, the reaction pathway between CO_2 and DME involves two separate reactions with methanol formed as the main intermediate. Taken separately, the two reactions require different types of catalysts to proceed effectively; the first step (CO_2 to methanol) involves a metal oxide catalyst (often Cu or Zn) that is usually supported by other metal oxides (ZrO_2, Al_2O_3, etc.) or noble metals (often Pd) [26], while the second step (methanol to DME) requires an acidic catalyst such as a zeolite (e.g. ZSM-5, MOR) or other solid acid catalysts (e.g. γ-Al_2O_3) [27–30]. In the following section, we will summarize the key related reaction mechanisms starting from the CO_2 to methanol reaction.

Table 1 Summary of catalyst studies

Catalyst	Prep. method	H_2/CO_2	GHSV ($ml/g_{cat}/h$)[a]	P, T (MPa, °C)	χ_{CO2} (%)	Υ_{CO} (%)	Υ_{DME} (%)	Reference
CuO–ZnO–Al_2O_3/HZSM-5	PM	10	10,471/h	36, 300	96	0.96	85.4	[18]
CuO–ZnO–Al_2O_3/HZSM-5	PM	3	3000	5, 260	29	33	65	[37]
CuO–ZnO–Al_2O_3/NaHZSM-5	CP	8	33.33 (g_{cat}) h/mol_{reac}	4, 275	51.0	8.2	36.0	[38]
CuO–ZnO–Al_2O_3–La_2O_3/HZSM-5	PM	3	3000/h	3, 250	43.8	11.8	31.2	[70]
CuO–ZnO–Al_2O_3/HZSM-5 + CNTs	PM	3	1800	3, 262	46.2	8.9	20.9	[39]
CuO–ZnO–Al_2O_3/Amorphous Si–Al	CP	3	1800	3, 266	47.1	12.3	20.1	[40]
CuO–ZnO–ZrO_2–V/HZSM-5	CP	3	4200/h	3, 270	32.5	9.1	19.1	[71]
CuO–Fe_2O_3–ZrO_2/HZSM-5	PM	5	1500	3, 260	28.4	2.2	18.3	[72]
CuO–ZnO–ZrO_2/FER	CP	3	8800	5, 280	29	7.0	18.1	[41]
CuO–ZnO–Al_2O_3/γ-Al_2O_3	CP	8	33.33 (g_{cat}) h/mol_{reac}	4, 275	40.0	7.6	16.0	[38]
CuO–ZnO–ZrO_2/FER	CP	3	8800	5, 260	26	8.2	14.5	[42]
CuO–ZnO–Al_2O_3–ZrO_2-Pd/HZSM-5	CP	3.3	1800/h	3, 200	18.7	2.4	13.7	[19]
CuO–ZnO–ZrO_2/MOR	CP	3	8800	5, 280	26	9.9	13.5	[41]
CuO–Fe_2O_3–CeO_2/HZSM-5	PM	4	1500	3, 260	20.9	5.2	13.2	[73]
CuO–ZnO–ZrO_2/MOR	CP	3	8800	5, 260	23.2	8.8	11.8	[42]
CuO–ZnO–ZrO_2/MFI	CP	3	2500	5, 240	23.6	5.8	11.6	[43]
CuO–ZnO–ZrO_2/FER	CP	3	8800	5, 260	23.5	9.6	10.8	[44]
CuO–ZrO_2–PdCNTs/HZSM-5	CP	3	25,000	5, 250	18.9	6.4	9.8	[74]
Cu–Mo/HZSM-5	IM	3	1500/h	2, 240	12.4	2.0	9.5	[75]
CuO–Fe_2O_3–CeO_2/HZSM-5	PM	4	1500	3, 260	18.1	4.6	9.4	[76]
CuO–Fe_2O_3–La_2O_3/HZSM-5	PM	4	1500	3, 260	17.2	5.2	8.8	[76]
CuO–ZnO–ZrO_2/MFI	CP	3	8800	5, 260	21.3	9.9	8.6	[42]
CuO–ZnO–ZrO_2/H–Ga–Sil	CP	3	1200	3, 250	19	6.4	8.6	[45]
CuO–ZnO–ZrO_2/WO_x–ZrO_2	CP	3	4333	3, 260	21.5	13.91	6.9	[46]
CuO–ZnO–Al_2O_3–ZrO_2/HZSM-5	WM	3	3100	3, 260	24.1	7	6.4	[47]
CuO–ZnO–ZrO_2/SO_4^{2-}–ZrO_2	PM	3	15,000	2, 260	17.19	11.9	4.4	[48]
PdZn/ZSM-5	PM	3	3500/h	2, 270	14	9.1	4.3	[6]
CuO–ZnO–Al_2O_3/γ-Al_2O_3	PM	3	3000	5, 260	15	82	3	[37]
CuO–ZnO–Al_2O_3/TPA + MCM-41	PM	3	40,000	4.5, 250	8.9	–	2.1	[49]

Notable catalyst studies including method of preparation and reaction conditions ordered according to DME yield (%)

PM physical mixing, *WM* wet mixing, *CP* co-precipitation, *IM* impregnation

[a]Unless otherwise specified

4 Catalyst Reaction Mechanisms

4.1 *CO_2 to Methanol*

The reaction of CO_2 to produce methanol—the first half of the reaction pathway to DME—is currently implemented on an industrial scale with the use of a Cu–ZnO–Al_2O_3 catalyst [31–33]. The mechanism of CO_2 to methanol involves three possibilities based on the intermediates formed. The most accepted and experimentally validated mechanism for the hydrogenation of CO_2 to methanol involves formate ($HCOO^-$) as the predominant intermediate. It follows a Langmuir–Hinshelwood mechanism in which both the CO_2 and H_2 molecules are first adsorbed and proceed to react through the formate intermediate en route to the final product of methanol. The entire mechanism is composed of eight main steps (g: gaseous, a: adsorbed) [31]:

1. $H_2(g) \rightarrow 2H(a)$
2. $CO_2(g) \rightarrow CO_2(a)$
3. $CO_2(a) + 2H(a) \rightarrow HCOO(a) + H(a)$
4. $HCOO(a) + H(a) \rightarrow H_2COO(a)$
5. $H_2COO(a) + H(a) \rightarrow H_2CO(a) + OH(a)$
6. $H_2CO(a) + H(a) \rightarrow H_3CO(a)$
7. $H_3CO(a) + H(a) \rightarrow CH_3OH$
8. $OH(a) + H(a) \rightarrow H_2O$

The rate determining step is the hydrogenation of $HCOO^-$ to H_2COO as this has the highest activation energy of the mechanism (Fig. 3) [34].

The second proposed mechanism involves the utilization of the RWGS reaction in which CO acts as the main intermediate in the pathway to form methanol [35]. This mechanism involves the initial adsorption of a HOCO species that binds to the surface of the catalyst through a single O atom, as compared to the two O atoms in the case of the formate intermediate. As a result, the adsorbed HOCO species is less stable than that in the formate pathway and is less favored. However, calculations have predicted that the formate species may poison the surface of the catalyst over time, resulting in an increased use of the CO pathway instead [31]. Additionally, the formyl (HCO^-) intermediate that is part of the CO pathway was observed to be quite unstable and prefers to dissociate back into CO and H_2, indicating that this pathway occurs on a much smaller scale than that of formate.

The third and more recent mechanism is proposed to occur via the formation of trans-COOH in place of $HCOO^-$ on the surface of the catalyst due to the presence of H_2O formed on the catalyst surface from both the RWGS and CO_2 to methanol reactions [36]. Observations concluded that the presence of water lowered the activation barrier associated with the formation of trans-COOH and thus indicated the formation of trans-COOH as being more thermodynamically favorable than the HCOO pathway.

The hydrogenation of CO_2 to methanol requires a transition metal catalyst supported on a metal oxide. Copper is the most commonly found catalyst used in this reaction, and Zn or ZnO supports are commonly seen as well. It has been experimentally shown that Cu on its own can catalyze the reaction, but the presence of Zn and ZnO significantly increases the production of methanol [33]. Studies have shown that Cu catalysts with Zn/ZnO supports are preferable for the $HCOO^-$ mechanism [31]. Fujitani et al. studied the effects of Zn on catalysis with Cu to determine the presence of active sites [37]. Experimental results concluded that metallic Cu was the main active site for the formation of $HCOO^-$ from CO_2, but Cu on its own was not enough to catalyze the reaction further. The addition of Zn facilitated the hydrogenation of $HCOO^-$ by stabilizing the molecule and providing support for further addition of H atoms, indicating that the Cu–Zn sites were key in the completion of the reaction through the formate pathway. It was also seen that the presence of Zn resulted in the formation of ZnO sites which additionally increased the rate of production of

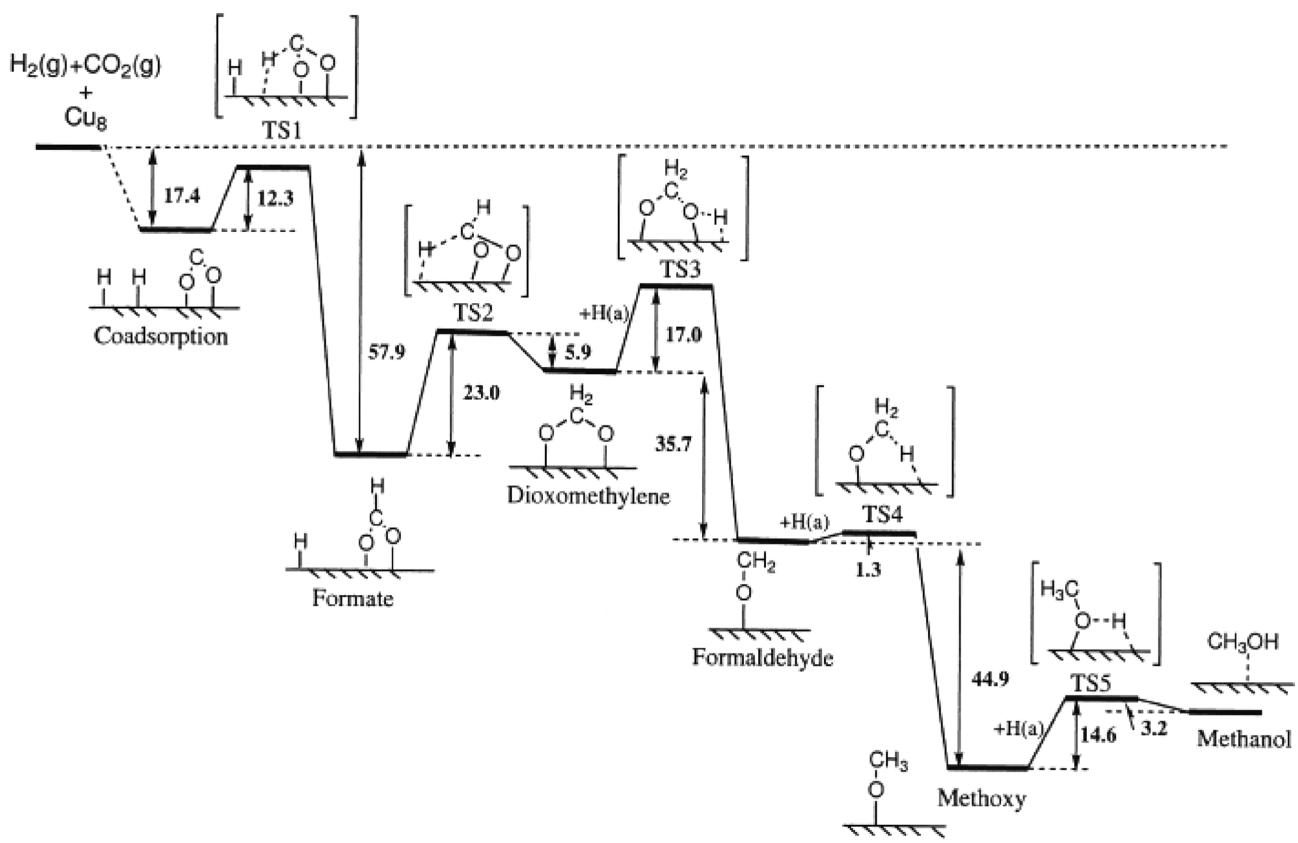

Fig. 3 Reaction mechanism for the formate pathway of CO_2 hydrogenation to methanol

methanol, indicating that surface O atoms may also play a role in further catalytic activity [32, 37]. While metallic Cu (Cu^0) is the main factor in initially catalyzing the CO_2, it is also believed that Cu^+ sites potentially contribute to increased methanol production [37].

4.2 Methanol to DME

DME synthesis from methanol requires an acidic catalyst such as a zeolite or γ-Al_2O_3 as the acidic hydroxyl groups on the surface of the catalyst are utilized for the dehydrative coupling of methanol over acid sites. Past production of DME has often occurred with liquid methanol as the reactant, but the use of gaseous methanol has become more widely accepted due to higher efficiency and better economic feasibility [38]. Several reaction mechanisms have been suggested to produce DME from methanol [38, 39] over the acid sites of zeolite/acid catalysts. While no single route has been proven accurate, three main mechanisms are currently accepted as potentially occurring in the reaction.

The first and most probable mechanism for zeolite-like catalysts (**A**) involves the associative adsorption of methanol molecules on bridging hydroxyl groups through hydrogen bonding (Fig. 4). These bridging hydroxyl groups between Al and Si atoms are typical of surface Brønsted acid sites (BAS) on zeolites and allow for multiple gaseous methanol molecules to hydrogen bond and in turn interact with each other to produce DME and water [38].

Another mechanism (**B**) has been proposed for zeolites, alternatively involving the dissociative adsorption of methanol molecules through dehydration and the formation of methoxy groups bonded to the oxygen atom of surface hydroxyl groups (Fig. 5). The methanol molecule displaces the proton of the hydroxyl group to form water and a surface methoxy group. This then reacts with another methanol molecule to form DME as a product and reform the surface hydroxyl group [38].

The final proposed mechanism (**C**) is more applicable to other catalysts such as γ-Al_2O_3 in which acid sites are often terminal hydroxyl groups (Fig. 6). This pathway again details the dissociative adsorption of methanol molecules which begins through hydrogen bonding and leads to the formation of a surface methoxy group on an open Al atom and the displacement of the entire hydroxyl group to form water. This methoxy group reacts with another methanol molecule to form DME and the remaining hydroxyl group attaches back to the surface in the terminal position [38].

Both mechanisms **A** and **B** are possible in zeolite-catalyzed reactions involving BAS, but theoretical calculations have shown that the associative pathway **A** is much more likely to occur and thus is highly favored due to the significantly endothermic nature of mechanism **B** [40]. It has been shown that hydrogen bonding occurs during the process, which again favors mechanism **A**, but surface methoxy groups have also been detected during the reaction, indicating mechanism **B** is still present to some degree [38]. Due to the generally different composition of γ-Al_2O_3 and

Fig. 4 (A) First proposed methanol to DME pathway (associative adsorption)

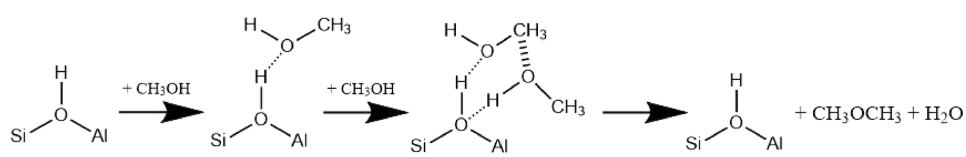

Fig. 5 (B) Second proposed methanol to DME pathway (dissociative adsorption)

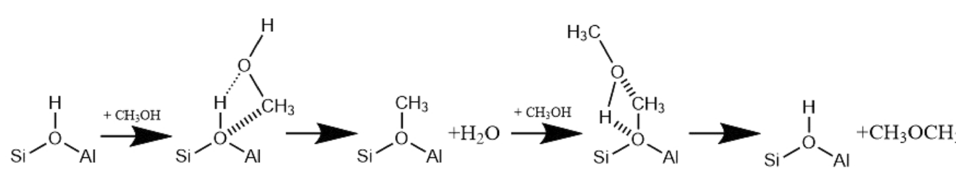

Fig. 6 (C) Third proposed methanol to DME pathway (terminal hydroxyl groups)

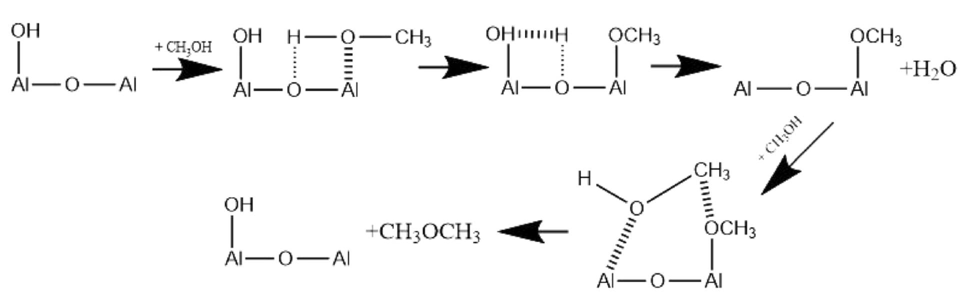

other similar catalysts with high concentrations of terminal hydroxyl groups and high Al content, the reaction is believed to occur mainly through the dissociative pathway **C** instead. In summary, the involvement of BAS on zeolites highly favors the associative pathway, while Lewis acid sites seen on alumina-based catalysts (γ-Al_2O_3) are much more likely to favor the dissociative pathway of methanol dehydration.

5 Catalyst Studies

Table 1 summarized some typical catalysts studied in this work.

5.1 Methanol Synthesis Catalysts

5.1.1 Metal Oxide

As previously mentioned, CO_2 hydrogenation to methanol often occurs over a Cu–Zn catalyst with common modifiers such as Zr and Al [24, 41–53]. The CuO–ZnO–Al_2O_3 catalyst combination is currently the most commonly utilized in industrial applications. The CuO–ZnO–Al_2O_3 and other metallic catalyst functions are mostly prepared by co-precipitation that is achieved through the use of aqueous metallic solution precursors that are combined and then precipitated into a single homogeneous solid. While the effect of Al on the catalyst is still not fully understood, it has been thought to act as a structural promoter that improves both catalyst morphology and stability. Additionally, it has been shown that Al^{3+} modifies the ZnO lattice structure by occupying substitutional sites [54]. It is reported the presence of Al^{3+} ions substitutes into the ZnO lattice and significantly improves conductivity, allowing for increased interaction with H_2 and O_2 molecules and thus a more efficient reaction.

Other promoters (Ga, Cr, etc.) have also been proposed for CO_2 hydrogenation in hopes of similar methods of action as has already been proven for Al [54, 55]. In particular, Ga^{3+} has shown promise in providing a similar promotional quality through the reduction of ZnO sites. While Al^{3+} (ionic radius of 0.39 Å) is incorporated into the ZnO lattice through substitutional sites, Ga^{3+} is present in a similar fashion through octahedral interstitial sites, as its larger ionic radius (0.47 Å) means it occupies a larger volume within the lattice structure. Both the Al^{3+} and the Ga^{3+} dopants result in a lowered reaction activation energy, facilitating the use of H_2 in the reaction as well as the adsorption of CO_2 and other intermediates through structural promotion [54].

Zr-promoted catalysts have also been studied to a larger extent than many others and are generally accepted to have greater performance than the traditional CuO–ZnO–Al_2O_3 catalysts [56, 57]. This increased performance is generally attributed to the lowered water adsorption induced by the weak hydrophilic nature of ZrO_2 and increased Cu dispersion seen after the addition of ZrO_2 into the catalyst lattice. Higher levels of Cu dispersion are correlated with a larger interaction and formation of Cu–ZnO active sites, theoretically increasing catalyst activity. Mn has been similarly studied as a catalyst additive by Ateka et al. in combination with SAPO-18 as the acidic catalyst function [56]. Both Zr and Mn doped catalysts showed higher performance than the traditional alumina, and Mn showed an even larger Cu dispersion effect than that of Zr, indicating promise for use as an additive (Fig. 7). The much lower cost of Mn nitrate as compared to Zr nitrate presents the possibility of the CuO–ZnO–MnO catalyst having an economical advantage in potential industrial implementation [56].

5.1.2 Noble Metals

The effect of noble metals (e.g. Rh, Au, Pd) on Cu–Zn catalysts has also been investigated [58–60]. Fierro et al. studied the effect of the addition of Pd to the Cu–Zn catalyst backbone through two precipitation methods for the production

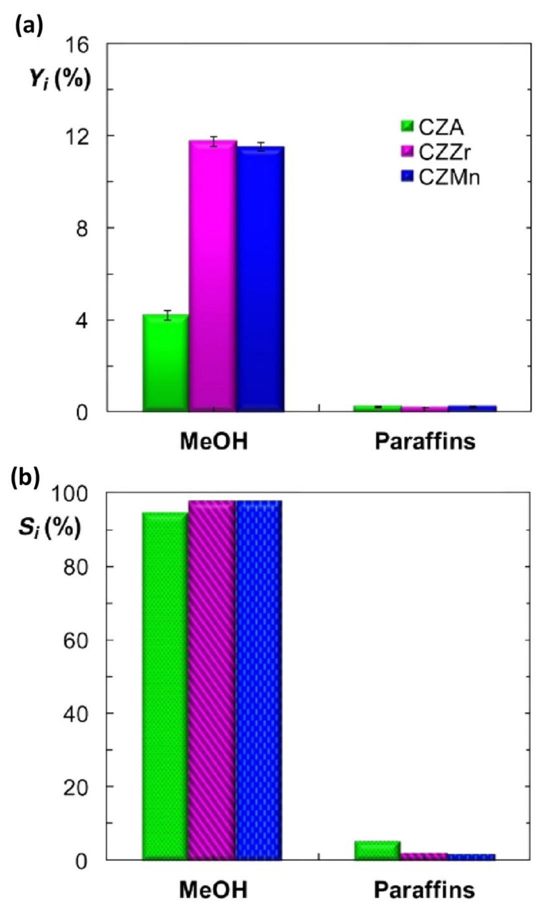

Fig. 7 Selectivity and yield of methanol for Zr and Mn modified catalysts [52]

of methanol from CO_2 [58]. It was shown that the co-precipitation method was quite detrimental to catalyst performance (most likely due to the difference in phases of the Cu and Zn precursors), but the sequential precipitation catalyst demonstrated improved methanol selectivity and yield compared to the base Cu–Zn catalyst [58]. Another study was done in regards to Au-doped Cu–Zn–Al catalysts in which a small amount of Au (1 wt.%) added through deposition–precipitation resulted in higher methanol yield (4.2% by mass) than the traditional catalyst without doping (3.75% by mass) [59]. Rh was also theoretically tested in place of Zn in a Rh–Cu catalyst alloy using density functional theory (DFT) calculations and modeling [60]. The models indicated CO_2 and intermediates adsorbed more easily in the presence of the Rh sites, suggesting higher performance compared to pure Cu (no comparison was made with Cu–Zn combinations however). In general, the addition of noble metals to Cu/Cu–Zn surfaces has been observed to have positive effects, with the success of many still not fully understood, but the high cost of materials may hinder this method's effectiveness in future practical applications.

Although Cu has been traditionally used in most applications of CO_2 to methanol production, problems with stability and sintering have prompted research on a number of non-Cu catalysts. Previous studies have been centered largely around noble metals supported on previously seen supports such as Zn and Zr [6, 61–63]. Pd is the most common noble metal used in such applications, with Pd–Zn combinations often taking the forefront of research [6, 61]. Although on the lower end, these catalyst combinations have shown methanol yield values comparable to other Cu-based catalysts [6]. Other supports have also been studied, such as the Pd–In_2O_3 catalyst synthesized by Rui et al. that achieved over 80% methanol selectivity and 14.4% yields [62]. Wu et al. reported Au supported on ZrO_2 at comparatively low temperature and achieved 73% methanol selectivity at 180 °C [63].

5.1.3 Non-noble Metal Bases

More recently, non-noble metals have been tested as catalyst bases for CO_2 to methanol, including Co, Mn, In, Ga, and Ni [64–70]. Cobalt (Co) is thought of as a promising alternative to noble metals due to its effect on limiting the RWGS reaction, with certain studies showing 0% selectivity to CO [64]. Co and Co–Mn combinations have drawn some attention but currently have not produced methanol selectivity and yield values that surpass those of noble metals [64, 65]. In_2O_3 has also been gaining traction as a potential substitute for noble metals due to its potentially similar RWGS-inhibiting action as Co and the formation of surface oxygen vacancies that result in active sites for CO_2 adsorption. A combination catalyst of In_2O_3–Co_3O_4 has promising CO_2 conversion and methanol selectivity that closely matches productivity of the Pd–In_2O_3 noble metal catalyst described above (methanol yield of just under 13% with 75–80% methanol selectivity) [69]. In_2O_3 has also been tested on ZrO_2 support as well as in combination with Ga [66, 67]. In_2O_3 impregnated on ZrO_2 had promising results with methanol selectivity of almost 80%, while In_2O_3 co-precipitated with Ga resulted in fairly low methanol yields [66, 67]. Ni was additionally integrated with Ga in one study and provided interesting results: approximately 100% conversion to methanol that was comparable to the original Cu–Zn combination. The presence of Ni itself was suggested to facilitate the RWGS reaction but it was poisoned by CO. The Ga sites promote only the conversion to methanol, and the poisoning of the Ni sites indicates the only prominent reaction is the creation of methanol from CO_2, meaning the overall prevalence of the RWGS reaction in this Ni–Ga catalyst is potentially less than that of the traditional Cu–Zn examples [68]. However, when Ni was combined with In_2O_3 and Al_2O_3 and promoted with different lanthanides, CO_2 conversion, and methanol selectivity were drastically lower in comparison [70]. The addition of lanthanides proved to increase catalyst productivity slightly due to a decrease in surface basic sites, but not enough to match the aforementioned or traditional catalyst combinations.

5.1.4 Carbon-Based Materials

Certain carbon-based materials such as nanorods and graphene aerogel are also being considered as potential supports and additives for the CO_2 to methanol catalysts [71, 72]. Zhang et al. detailed the formation of a polymer nanorod with Cu–Zn framework for effective formation of methanol with ideal metal dispersion and support.

Zeolitic imidazolate frameworks-8 (ZIF-8) was used as the primary template which was then impregnated with Cu and substituted with 1,3,5-benzenetricarboxylic acid (BTC) to create the desired nanorod structure. This nanorod structure resulted in a much less drastic decrease in methanol selectivity with an increase in temperature as compared to the co-precipitated Cu–Zn catalyst, and the catalyst demonstrated high stability even after 280 h of use [71]. Graphene oxide aerogel was also used as a support for the Cu–Zn catalyst due to the much larger surface area of graphene aerogel as compared to many other suggested supports (Fig. 8). Catalysts contained a wrinkled 3D lattice impregnated with Cu–Zn, resulting in very high surface area and thus a large number of active sites that largely increased methanol yield compared to other traditional catalysts [72].

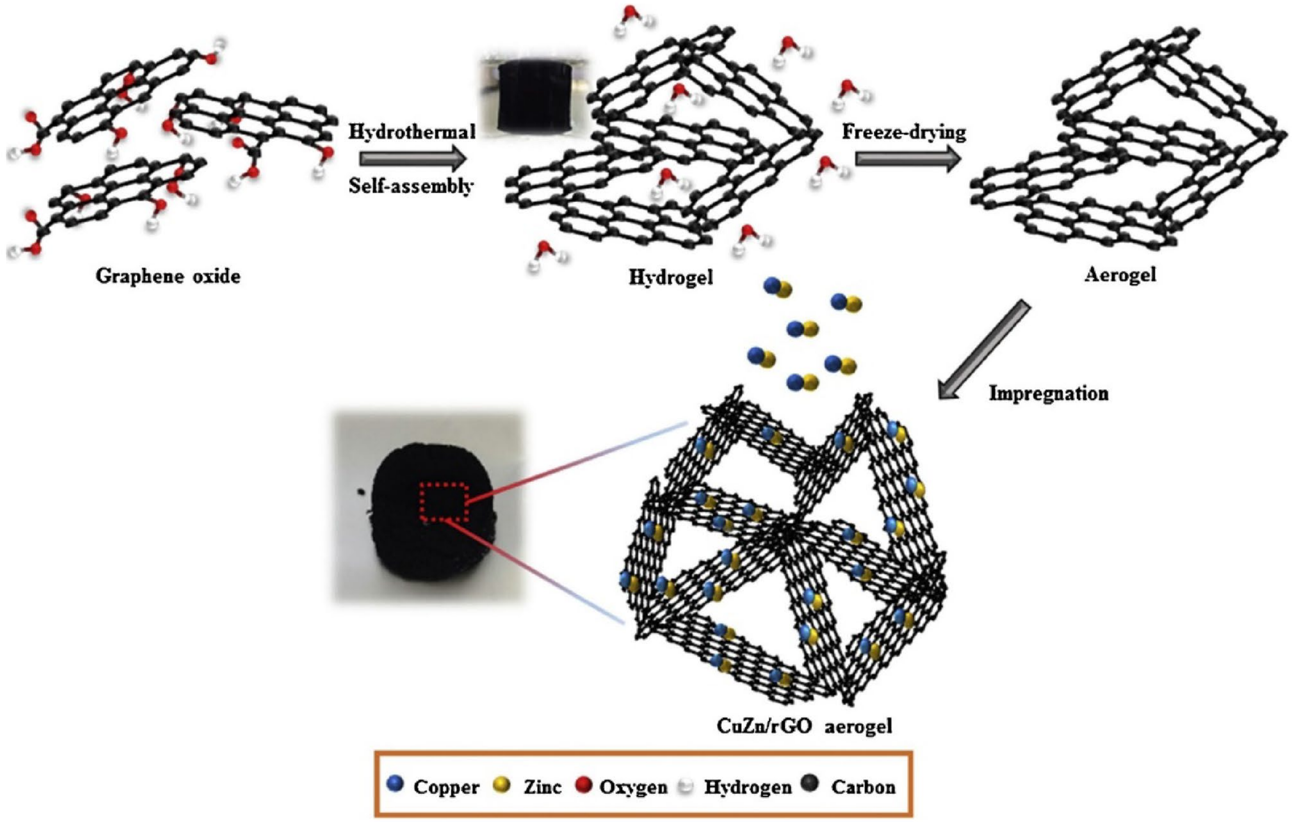

Fig. 8 Schematic for the production of Cu–Zn supported on graphene aerogel [68]

5.1.5 Metal–Organic Framework

Metal–organic framework (MOF) was also employed for methanol synthesis, for example, Cu enhanced MOF. Zr-based UiO-66 incorporating Cu via crystal encapsulation was further employed for methanol synthesis [73], which demonstrated 100% methanol selectivity but low overall yield due to poor CO_2 conversion of around 1.5%.

5.2 DME Synthesis Catalysts

5.2.1 γ-Al_2O_3

As mentioned previously, the second step of the reaction often takes place over acidic catalysts such as γ-Al_2O_3 or ZSM-5. Alumina-silicate based γ-Al_2O_3 is generally considered the "traditional" most commonly used catalyst for this step, as it possesses high surface area, good thermal stability, and the presence of weak- to medium-strength acid sites that facilitate the production of DME [41, 42]. γ-Al_2O_3 is also inexpensive and currently industrially used as a methanol-to-DME catalyst. However, γ-Al_2O_3 often requires high temperatures to produce high yields of DME, and the hydrophilic character of the catalyst results in water adsorption that effectively poisons the catalyst and results in a drop in productivity. As such, zeolite catalysts have been more recently suggested as replacements for the production of DME.

5.2.2 Zeolites

Zeolites are aluminosilicate based materials in the form of a lattice in which aluminate and silicate ions are bound with oxygen atom links. These materials contain pores which often facilitate the reactions by directing the reactants through the pore channels. Zeolites contain both Brønsted and Lewis acid sites, both of which can facilitate the dehydration of methanol to DME, but Lewis acid sites are generally more successful due to their lower overall acidity (less harsh conditions). These porous materials often have high surface areas which has a positive effect on the DME yield. The most commonly suggested is ZSM-5, often presented in the H-form [6, 24, 25, 41–43, 51, 74–80]. The choice between γ-Al_2O_3 and HZSM-5 is often debated since HZSM-5 has less hydrophilic character and thus is not majorly affected by the adsorption of water; however, the zeolite's stronger acidic sites sometimes result in the formation of hydrocarbon byproducts and coke deposits that may hinder overall productivity.

Many studies have been done with the final goal of improving the productivity and physical properties of ZSM-5 and other zeolites. For example, HZSM-5 and other zeolites were halogenated with either fluorine or chlorine (in an attempt to increase acidity) and subsequently subjected to ultrasonic irradiation to investigate the effects of halogens and irradiation on catalyst performance [81]. It was found that the impregnated catalysts had improved DME yield with both chlorine and fluorine compared to the base zeolites due to an increase in the number of BAS (chlorine or fluorine preference depended on the specific catalyst). Additionally, ultrasonication generally improved DME yield for all chlorinated catalysts but not as much for the fluorinated counterparts, most likely due to increased surface area and pore volume on the chlorinated catalyst combinations.

Other zeolites such as FER-, MFI-, and MOR-type catalysts have been studied as alternatives with various results [45–48]. The FER-type catalysts have generally demonstrated higher productivity than the other two (attributed to a more uniform surface spread of metal oxides as well as higher acid capacity), with DME yield of up to 18.1%. Following the zeolitic catalyst trend, water adsorption was insignificant, and the FER catalysts in particular have shown less coke formation as a whole when compared to others [45–48].

5.2.3 Heteropolyacids

Heteropolyacids (HPAs) have been gaining attention as acidic function catalysts due to their high Brønsted acidity, allowing for higher productivity and catalytic activity at lower reaction temperatures (Fig. 9) [82–88]. HPAs most commonly has the form $H_nXM_{12}O_{40}$ where X is the heteroatom (P^{5+} and Si^{4+} are common), and M is a transition metal (typically Mo^{6+} or W^{6+}). Since HPAs have very low comparative surface areas, they are often supported on another material such as TiO_2 or boron nitride (BN) to increase surface area and thus also catalytic activity. $H_3PW_{12}O_{40}$ (HPW) and $H_4SiW_{12}O_{40}$ (HSiW) take the forefront of HPA research, with TiO_2, SiO_2, and ZrO_2 being the most effective supports on which these HPAs are implemented. Alharbi et al. investigated both HPW and HSiW on SiO_2 and TiO_2 supports [84]. In general, HPW showed slightly higher conversion and SiO_2 provided the most effective support, with the higher surface area being directly correlated to increased methanol conversion. The most successful catalyst achieved 24% methanol conversion (surface area of 213 m^2/g), DME selectivity of all combinations remained at 100%. In a support-oriented study, HSiW was solely tested on six different support surfaces in comparison to the bulk acid [85]. TiO_2, SiO_2, and ZrO_2 were proven more effective catalyst supports, with TiO_2 and SiO_2 claiming higher methanol conversion but with TiO_2 and ZrO_2 showing higher DME production rates overall (highest methanol conversion was 90% and all catalysts demonstrated 100% selectivity for DME). As expected, the supported HPAs were more effective than the bulk catalysts due to higher surface area and better dispersion of HPA unit sites. When compared to γ-Al_2O_3, HPA productivity was drastically higher at its most effective temperature, as the alumina-based catalyst requires higher temperatures (above 200 °C) while HPAs function best at lower temperatures (180–200 °C). A study on different HPA loadings solely on TiO_2 was done with both HPW and HSiW catalysts, concluding that an HPA loading of

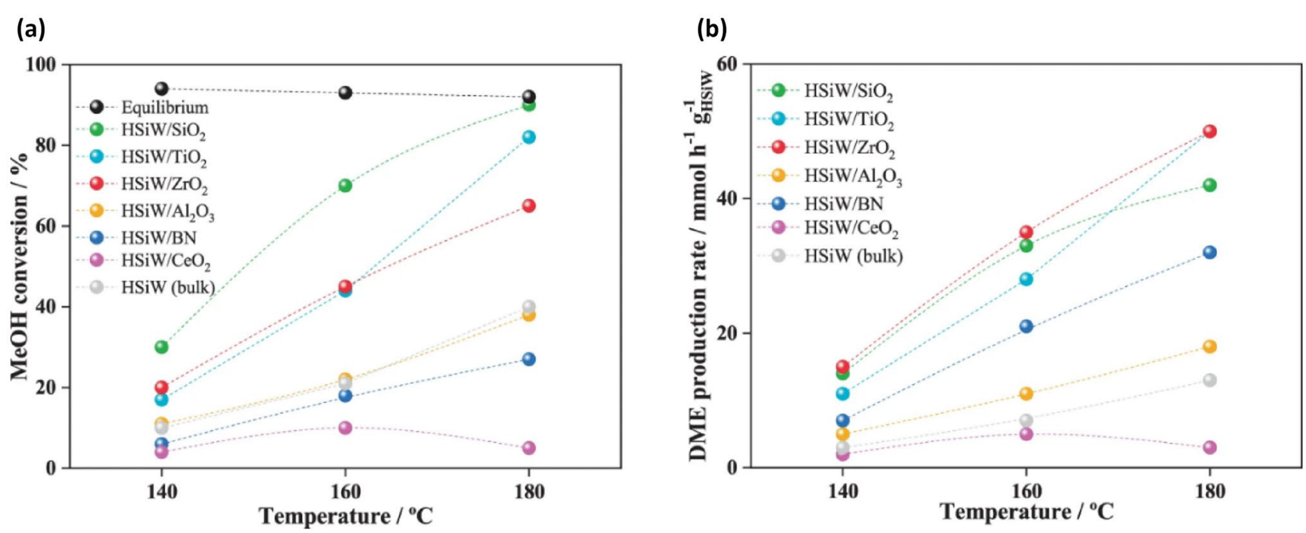

Fig. 9 Methanol conversion and DME production for different HPA supports [81]. (https://creativecommons.org/licenses/by/4.0/legalcode, no changes made)

around 4.5 HPA units/nm^2 had the highest methanol conversion for both of the investigated HPAs [83]. In contrast, Schnee et al. focused on BN as a support for HPW catalyst in comparison to the TiO_2 support [82]. It was discovered that the HPW interacts differently on the surface of the BN as compared to the TiO_2, forming exclusively strong acid sites on the BN in contrast with the majority medium strength acid sites on the TiO_2 surface. This resulted in higher overall activity on the BN-supported catalyst, indicating more options to be investigated as an alternative for the more commonly used supports (e.g., TiO_2).

5.2.4 Silicoaluminophosphates

In a matter more similar to zeolites, certain silicoaluminophosphate (SAPO) catalysts have been experimentally implemented as the acidic catalyst function in this reaction process [89, 90] (e.g. SAPO-18, SAPO-34, etc.), but the most promising as of the present is SAPO-11. This catalyst contains micropore volume of 0.0498 cm^3/g and weak acidic sites that promote the production of DME without hydrocarbon or coke formation [90]. When studied in comparison to other SAPO catalysts (SAPO-18), SAPO-11 demonstrated a significantly higher yield of DME in the ideal reaction temperature range due to high density of weakly acidic sites and a porous structure that limits coke or hydrocarbon formation. Additionally, SAPO-11 has been used in combination with CuO–ZnO–ZrO_2 metallic function for direct production of DME from CO_2 and had slightly higher value of DME yield (~7.2%) and somewhat better stability than that of the tested control of CuO–ZnO–ZrO_2/HZSM-5 [90]. The performance of this SAPO-11 catalyst was even further enhanced with the discovery of a method to create nano-sized SAPO-11 crystals that result in more efficient DME production [89]. Ethanol was used as both a solvent and a growth modifier in order to grow smaller nano-SAPO-11 crystals. The smaller-sized catalyst results in a larger surface area on which the reaction can be further promoted, resulting in better productivity than both the traditional (micro) SAPO-11 catalyst as well as γ-Al_2O_3 examples. The nano-SAPO-11 had much higher methanol conversion (80%) at lower temperatures (~290 °C) and continued this high level of conversion over a larger temperature range (290–400 °C) than both the micro-SAPO-11 as well as the γ-Al_2O_3. DME selectivity was comparable between all three at lower temperatures, but the nano-SAPO-11 was also characterized by maintaining higher selectivity over a broader temperature range than both other catalysts [89].

5.2.5 Other Silica-Based Materials

Certain silica-based materials have been suggested as additives for typical zeolite catalysts like HZSM-5. A noticed issue with HZSM-5 as a catalyst is its microporous structure: it contains micropores (~0.5 nm) that are subject to decreases in reaction rate due to blockage with reactants and by-products [91]. Because to the diameter of the pores being similar to the size of the molecules, diffusion of the reactants and formed DME is limited, and catalytic activity is lost over time. Thus, materials that have somewhat larger pore sizes would be more suitable for DME synthesis over longer reaction times. One such proposed material is the silica-based MCM-41. This material, however, comes with disadvantages of its own, such as very low acidity. Tang et al. proposed a solution to this by integrating MCM-41 with HZSM-5 to create a molecular sieve that could promote a better pore size distribution while maintaining a reasonable level of acidity from the HZSM-5 [91]. When tested in parallel with pure HZSM-5, it was shown that conversion and selectivity with the zeolite alone dropped significantly over time and with an increase in temperature, while the MCM-41/HZSM-5 hybrid maintained conversion and selectivity incredibly well over the same measures, bringing forward a suitable method for increasing HZSM-5 stability and lifetime.

Similar to HPAs mentioned above, some attempted combinations of acidic catalysts involve the main substituent supported onto another material, primarily ZrO_2. The most plausible combinations often include SO_4^{2-} or WO_x compounds [50, 52, 92, 93]. Sulfonated zirconia is the most commonly seen out of these two combinations due to the generally strong acidity of SO_4^{2-} when supported on ZrO_2. Witoon et al. investigated the effects of sulfur loading on the sulfonated zirconia catalysts to identify the tendencies of SO_4^{2-} on the ZrO_2 surface [92]. At lower sulfur contents, it was shown that the sulfate-induced the zirconia surface into acting as weaker Lewis acid sites, while higher sulfur contents resulted in protonated sulfates acting as stronger BAS. The weaker acid sites on the lower sulfur loadings were more active at higher temperatures, but the stronger acid sites for higher sulfur loadings resulted in much higher catalytic activity, with 20 wt.% having the highest DME yield overall at 260 °C. Temvuttirojn et al. supported SO_4^{2-} onto high surface area mesoporous ZrO_2 to increase the catalyst surface area [52]. Although still on the lower end, this method produced a 4.4% DME yield with quite successful catalyst stability.

5.2.6 Metal Oxide Supports

WO_x compounds have been supported similarly in several studies [50, 93]. The WO_x compounds do not afford the same acidic ability as the SO_4^{2-}, but when supported on ZrO_2, the W groups are often more stable and more resistant to interactions with water during the reaction. The WO_x/ZrO_2 combination was studied in parallel with the traditional CuO–ZnO–ZrO_2 for the direct production of DME from CO_2

and demonstrated a reasonable DME yield of 6.9%, higher than that of the SO_4^{2-} catalysts [50]. Additionally, the catalysts had very high stability, with practically no decrease in production over 48 h. In a different approach, WO_x was instead supported on an unmodified Al_2O_3 acidic catalyst and again combined with CuO–ZnO–ZrO_2 for the direct reaction [93]. Unfortunately, this combination only produced a 2.9% DME yield and lowered stability due to coke formation and the adsorption of water.

Niobium oxide acid catalysts have also been attempted [94]. Niobic acid has been proven to act as an effective acid catalyst in certain reactions, and the dispersion of different niobium oxides on supports tends to form distorted octahedral and other geometric structures that favor the formation of both Lewis and BAS. A study analyzed different niobium loadings in a Nb/TiO_2 catalyst for methanol dehydration which yielded the highest values of 11.3% CO_2 conversion and 93% DME selectivity at the highest loading [94].

5.2.7 Methyl Carboxylate Esters

Interestingly, one study detailed the addition of different methyl carboxylate esters as promoters in the methanol-to-DME reaction [95]. Ester chain length was changed in the experiment to investigate the effects of longer chained esters on the reaction productivity, and all esters from methyl formate to methyl *n*-heptanoate were employed. It was shown that the esters did not interfere with the reaction and instead were very efficient promoters to increase DME yield. As chain length was increased, DME yield was also increased for all acidic catalyst examples (HZSM-5, H-MOR, etc.), with methyl *n*-hexanoate reaching ~22% methanol conversion at upwards of 99% selectivity to DME. This reaction also proved thermodynamically intriguing as it was conducted at 150 °C (423 K), a much lower temperature than is generally required for all other catalysts mentioned. As chain length increased further, there was no discernable increase in DME production. Using the esters as promoters was proven even more advantageous because the specific esters can be switched easily with no unwanted effect on the reaction due to the readily reversible nature of the promotion (Fig. 10).

5.2.8 Mineral Clays

As a final category of acid catalyst options, there have been several studies that investigate the use of mineral clays for the conversion of methanol to DME [96–98]. In general, these clays come in the form of natural zeolites such as kaolinite or diatomite. The zeolite-like composition of these clays resulted in similar activity compared to the zeolites that are used industrially. Although kaolinite and diatomite have been tested without modifications as catalysts, results have been reported lower reactivity motivating research for supported and enhanced clay catalysts. Of note, kaolinite clay was impregnated with different loadings of cobalt and tested directly for the methanol-to-DME reaction. The catalyst showed promising methanol conversions of between 60% and 80% as well as DME selectivity of up to 95% (at 350 °C) [96]. From a more thermodynamically feasible standpoint, methanol selectivity was close to 25% with 100% DME selectivity at 250 °C. While not geared for the production of DME as this paper entails, another study was conducted in which CuO–ZnO was supported on kaolinite and then physically mixed with SAPO-34 for the direct conversion of CO_2 to light olefins [97]. The composition of this catalyst is very

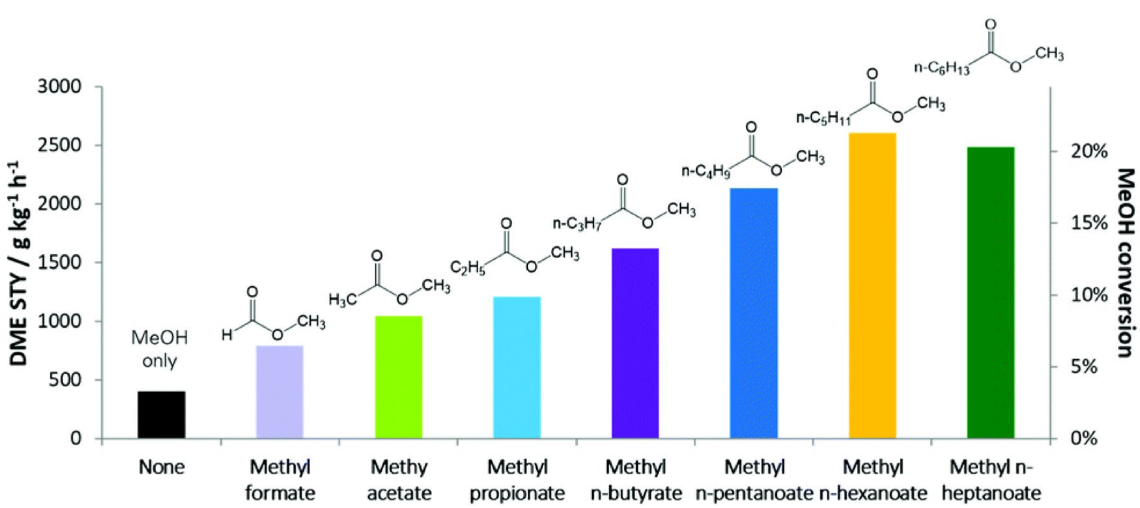

Fig. 10 DME yield and methanol conversion of mixed feeds of methanol and different methyl carboxylate esters [95]

similar to those employed for CO_2 to DME reactions, and the promising yield of 20–40% indicates that similar catalysts could be devised for the DME pathway as well.

5.3 Miscellaneous

To minimize the negative implications of the formation of water on catalysts in the reaction system, a different approach has also been proposed which entails a membrane-fitted reactor, in turn allowing for more optimized catalyst performance. Rodriguez-Vega et al. created a membrane reactor setup that utilized an LTA zeolite membrane for the elimination of water and by-products from the reaction chamber [99]. The reaction employed a physically mixed CuO–ZnO–ZrO_2/SAPO-11 and achieved DME yields of 15–20%. The membrane reactor demonstrated effective elimination of water that allowed for higher catalyst performance than the same reaction setup run identically without the membrane, indicating promise as an alternative setup for the CO_2 to DME reaction.

6 Bifunctional and Hybrid Catalyst Systems

The preparation of the catalyst for the hydrogenation of CO_2 to DME plays a crucial role in the scalability of the reaction for industrial applications. As the reaction generally takes place in two steps with methanol as the intermediate, there have been several applied techniques for the combination of the two catalyst functions into a single working catalyst for a one-pot synthesis. As mentioned earlier, a single bed with the use of the combined catalyst helps lower operating and capital costs and improves efficiency as compared with a multi-bed reactor system. Moreover, the integration of metal and acid sites into one catalyst reduces thermodynamic limitations in methanol synthesis which results to higher CO_2 conversions and DME selectivity. The current strategies for the combination of the metal and acid catalyst components can be separated into two categories: bifunctional and hybrid. The distinguishing factor between these two forms of catalysts is the physical or chemical combination between the two functions; in bifunctional catalysts, the metallic and acidic functions are physically mixed, while hybrid catalysts are chemically mixed (often through co-precipitation). Bifunctional catalysts contain dispersed acid and metal active sites that are not in direct contact with each other, thus maintaining the two-step process of CO_2 to methanol and subsequently methanol to DME. In comparison, closer contact of metal and acid sites is characteristic of hybrid catalyst combinations and the two often work in parallel to create a "one-step" reaction in which CO_2 is converted practically directly to DME due to the two reaction steps working concurrently in very close proximity.

6.1 Bifunctional Catalysts

The most commonly applied method of producing bifunctional catalyst is physically mix the metal and acid catalyst (HZSM-5, γ-Al_2O_3, etc.) to form a combination powder catalyst that can be pelletized for convenience. Since no chemical reaction occur during the mixing process, more active sites can be exposed and well dispersed using this method. As the most used bifunctional catalysts preparation method, it has been studied further than other examples of catalyst combinations. Physically mixed catalysts have demonstrated the highest DME yield overall (as shown in Table 1) [24, 41]. CuO–ZnO–Al_2O_3/HZSM-5 mixture shows the best performance with DME yield of 85.4% but required high temperature and high pressure (see Table 1), which is the main obstacle stopping the possibility of industrial application [24]. However, other tests with similar physically mixed catalysts have shown DME yield of up to 65% with milder reaction temperatures and pressures (5 MPa, 260 °C) [41] (Fig. 11).

A unique method of bifunctional catalyst synthesis has also been developed, involving a core–shell capsule design in which one of the catalyst functions is the core and is coated with the second function that acts as the shell [100–104]. These catalysts can be prepared through different methods such as physical coating, impregnation, surface infiltration, and hydrothermal synthesis, where either the metallic function acts as the core [100, 101, 103], or the inverse in which the acidic function is coated with the metallic [102, 104]. The design of the core–shell catalysts promotes a synergetic

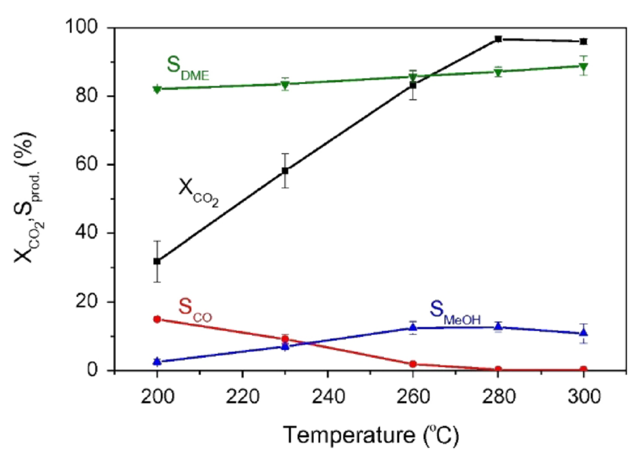

Fig. 11 CO_2 conversion and DME selectivity for physically mixed CuO–ZnO–Al_2O_3/HZSM-5 (highest recorded catalyst DME yield) [18, 23]

combination of metal and acid active sites that improves the catalyst function more than the traditional physically mixed counterparts.

MOF were also tested in a bifunctional catalyst system in which silicotungstic acid (STA) was supported on UiO-66 MOF and physically mixed with Cu for the conversion of syngas to DME. While the method was plausible (1.99% CO conversion and 69.3% selectivity to DME), the overall yield was still less than that of the baseline Cu–ZnO/γ-Al_2O_3 physically mixed counterpart (10.15% CO conversion and 43.02% selectivity to DME) [105].

6.2 Hybrid Catalysts

Although more recently implemented, hybrid catalysts for the conversion of CO_2 to DME have gained more traction as of the present day. Despite the growing interest and utilization of these hybrid catalysts, progress in their studies has been slower due to the increased importance of the chemical composition of hybrid catalysts. Due to the proximity of the metal and acid sites, the correct ratio must be achieved to develop the desired dispersion and surface properties that these active sites can afford. Hybrid catalysts are often synthesized using different methods of precipitation or impregnation to chemically incorporate both functionalities into a homogeneous catalyst. Hybrid catalysts for DME production from CO_2 have not yet achieved DME yields comparable to those of the best physically mixed catalysts but have successfully demonstrated DME yield of up to 36% with reasonable reaction conditions (4 MPa, 275 °C) [42]. This CuO–ZnO–Al_2O_3/NaHZSM-5 catalyst also had the positive characteristic of relatively low CO production as a by-product (8.2%). Other co-precipitated catalyst combinations reached DME yields of around 20% [44, 75]. When comparing co-precipitation with deposition, results are generally mixed and depend on the specific catalyst being used.

In order to improve the spread of the active sites within hybrid catalysts, carbon nanotubes have been studied as supports through precipitation methods with both functions of the combined catalyst [43, 78, 106]. These carbon nanotubes (Fig. 12) allow for a more uniform surface characterization due to their nature as effective supports, which allows for a more productive connection between the more dispersed metal and acid active sites. The carbon nanotube catalysts synthesized through co-precipitation of both metallic and acid functions in parallel with the nanotubes show competitive DME yields (9.8%) when modified with Pd [78]. Although the final catalyst was physically mixed, another study detailed a CuO–ZnO–Al_2O_3/HZSM-5 catalyst in which both the metallic and acidic functions were separately co-precipitated with carbon nanotubes before being physically mixed together [43]. This catalyst outputs a remarkably high DME yield value of 20.9%, which was higher than that of the identically produced catalyst without the presence of nanotubes (Fig. 13).

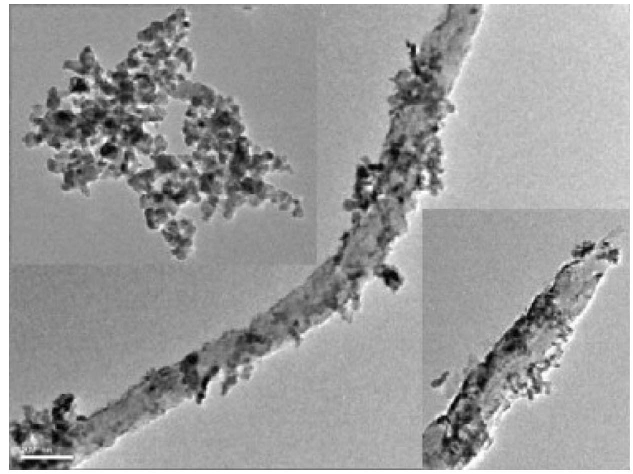

Fig. 12 Transmission electron microscopy image of CuO–ZnO–Al_2O_3 supported on carbon nanotubes [39]

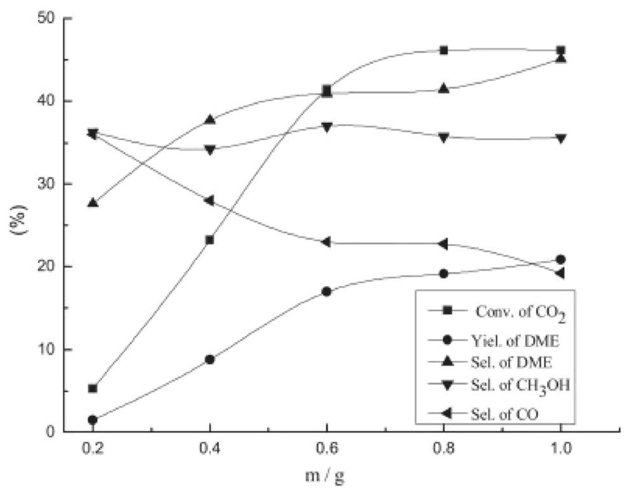

Fig. 13 CO_2 conversion, selectivities of products, and DME yield for carbon-nanotube-supported CuO–ZnO–Al_2O_3 at different catalyst masses [39]

HPA systems have also been employed for direct production of DME from CO_2 by combination with typical metallic catalysts [86, 87]. Millán et al. reported that lower loadings of HPW showed much lower DME yields than the typical CuO–ZnO–Al_2O_3/HZSM-5 combination, however, the 2.7 monolayered HPW exhibited a higher DME yield and a lower deactivation rate than that of the more established catalyst. In a different approach, HPW and $H_3PMo_{12}O_{40}$ (HPMo) were layered onto montmorillonite K10 clay as support and physically mixed with CuO–ZrO_2 metallic component for CO_2 to DME conversion [87]. The highest DME yield values were observed under HPW-combinations, but yields were still on the lower end when compared to the traditional zeolite/γ-Al_2O_3 catalysts (highest yields between 2% and 3%). Yu et al. studied a unique approach to HPA catalyst combinations, using Cu and Fe HPA salts [88]. Catalysts were synthesized through a simple replacement reaction and demonstrated 100% DME selectivity from methanol up to 250 °C (Fig. 14). All salts showed greater catalytic stability than the pure HPAs, with CuSiW and FeSiW salts showing the slowest deactivation and fairly high continued productivity (>65% methanol conversion) after 120 h. Taken together, HPA-based catalysts are very interesting candidates for DME production, as they have demonstrated potential for high DME yields as well as operation at lower temperatures, indicating a better potential outlook in industrial use.

7 Challenges

The method of combining the two catalyst functions for the direct conversion of CO_2 to DME presents new obstacles to large scale implementation, as the mixing of the two catalysts must be done very specifically in order to maximize production. The method of mixing, size of the metal particles, and the acidic catalyst used are all important factors that must be considered, as a change in any could drastically affect the production of DME [107].

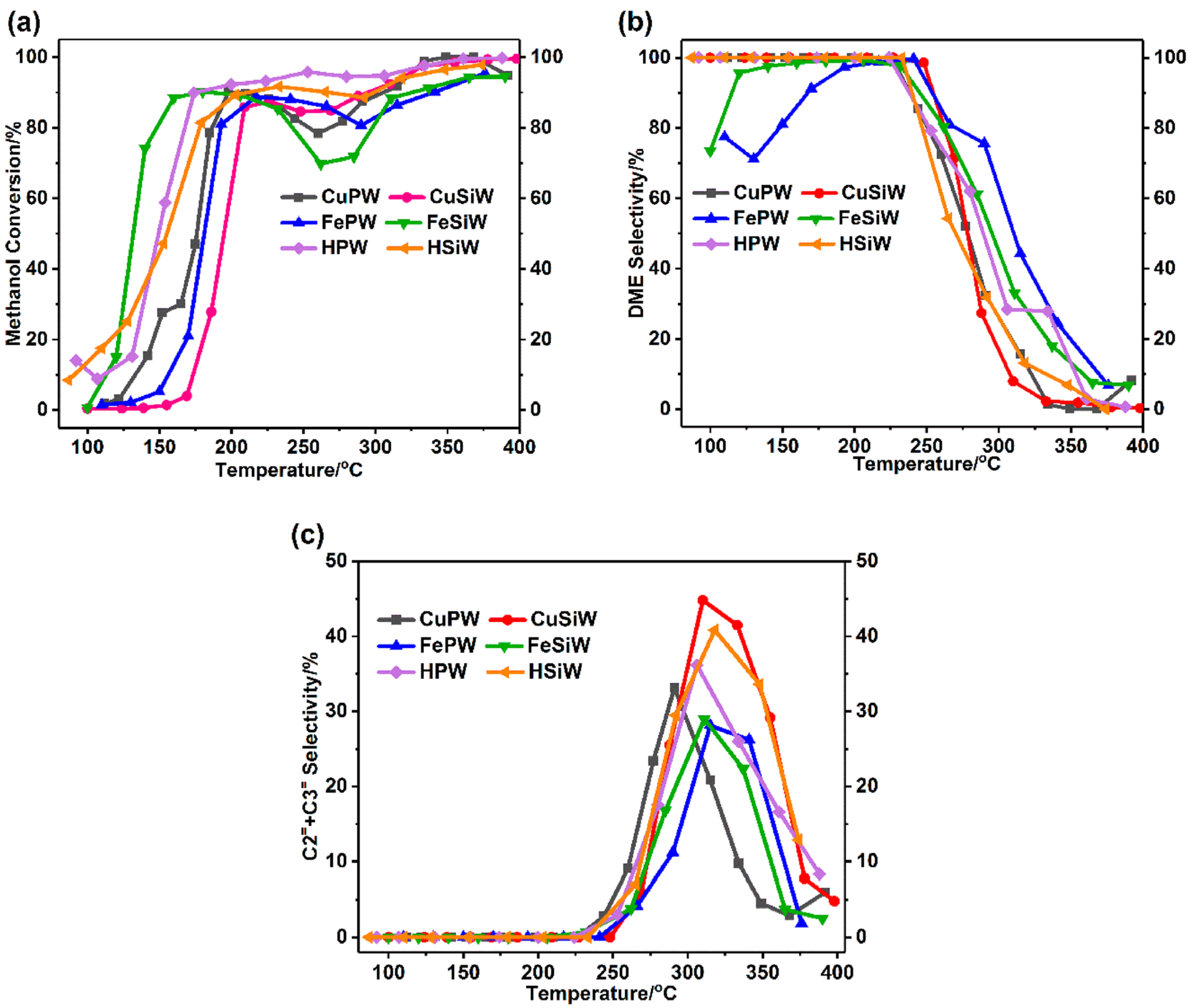

Fig. 14 Conversion and selectivities for Cu and Fe HPA salts compared to base HPAs [84]. (https://creativecommons.org/licenses/by/4.0/legalcode, no changes made)

A challenge that presents itself with the Cu-based catalysts for the methanol production step is the potential sintering of Cu and other metals at high temperatures. Cu has generally been shown to sinter at temperatures of over 300 °C and thus any reaction must be kept safely under this threshold to ensure the continued stability and production of this catalyst function over longer periods of time [108, 109].

The main challenge seen with zeolite-type catalysts such as ZSM-5 for the methanol to DME step is the potential deactivation over time due to coke deposits and ion migration. As mentioned previously, the microporous zeolite surface allows for molecules (by-products) to become trapped within the pore channels and deactivate the catalyst over time, possibly through coke formation or through pore blockage. When mixed with the metallic function, ion exchange between the metallic and zeolitic active sites is also possible, which has been seen to potentially impair catalyst activity [110]. However, the deactivation from ion exchange has been largely reported only when using metallic/zeolite mixtures for hydrocarbon/olefin formation and positive effects from the ion exchange have also been seen when using these catalysts for DME production [111].

Apart from catalyst stability, thermodynamic considerations must also be evaluated for DME production. All catalyst systems required temperatures of 200 °C and above to produce successful results, with the exception of the methyl carboxylate ester promoters, with higher temperatures and pressures generally correlating to higher DME yield. The challenge of implementing these catalysts (or newly discovered alternatives) at lower temperatures can drastically influence the outlook on feasibility of implementation.

8 Perspectives and Outlook

The combination of metal and acid functionalities into one catalyst offers improved thermodynamics in CO_2 hydrogenation. However, the low temperature requirement for high DME selectivity due to competing RWGS reaction also results in low catalytic activity. Hence, designing a catalyst with high catalytic activity at low temperatures is an important challenge to overcome. Performing computational studies (e.g., DFT calculations, micro-kinetic modeling, etc.) would be a promising research direction to aid in finding the optimal catalyst combinations for CO_2 to DME reactions. Additionally, significant insights on the reaction mechanisms and a deeper understanding of the role catalyst active sites could be obtained from these studies which would be beneficial in designing high-performance catalysts. It is also important to consider that the catalysts should be stable in the presence of water as hydrogenation and RWGS reactions produce significant amounts of water.

Looking at the metallic catalysts, most of the studies presented focused on the use of Cu-based catalysts. However, given the exothermic nature of the reactions coupled with the susceptibility of Cu to sintering, it is imperative to explore different synthesis techniques or catalyst configurations to minimize the catalyst deactivation. One possible method that can be further investigated is the encapsulation of the metal oxides in zeolites which may improve its stability and prevent sintering [112].

Ensuring the stability of the acidic catalysts is also critical for a high-performing catalytic system. Zeolites have been mostly used as the acidic site for the CO_2 hydrogenation to DME, but its porous structure makes it susceptible to coke formation, and thus deactivation. A study by Arora et al. [113] showed that high-pressure H_2 cofeeds minimizes coke formation in zeolites in methanol to hydrocarbons reactions. Similarly, this can be tested as well on CO_2 to DME reactions by changing H_2/CO_2 feed ratios. HPAs have also been shown to have slower deactivation rates compared to HZSM-5 and further improvements in its design to improve conversion and selectivity to DME could make it a promising acidic catalyst. The synergetic character of the active sites on hybrid catalysts has proven a very promising scope for the direct conversion of CO_2 to DME, but the correct chemical compositions must still be evaluated through further research to compete with the most productive physically mixed catalysts.

The use of data-driven computer modeling can also improve the experimental process over time by providing insight into reaction optimization and configuration. Reaction kinetic modeling has been attempted and results were very promising when experimentally validated afterwards [114].

In an industrial perspective, performing process optimization or intensification considering current catalysts combinations, conversions, selectivity to DME, and catalyst lifetimes would be beneficial in determining other factors/limitations that researchers must consider when designing their catalysts. Certain optimization processes such as recycling the water produced within this reaction to be used for electrolysis (and thus the production of more H_2) can add increased sustainability to the process and increase the merit of implementation. Additionally, an economic analysis of the CO_2 to DME industry would provide an outlook on the conversion and selectivity that must be targeted for a feasible and sustainable process.

9 Conclusions

Current progress on the combined catalyst system for CO_2 hydrogenation to DME has yielded promising DME yield values, with the highest at 85.4%. In general, extreme reaction conditions (36 MPa and 300 °C) could result in higher DME yield. Despite this, several catalyst combinations have demonstrated substantial production of DME even at milder reaction conditions, reaching up to 65% at 5 MPa and 260 °C. Utilizing milder reaction conditions is pivotal to realizing the potential of CO_2 to DME conversion as an industrial process to reduce operational costs. As a whole, the CuO–ZnO–Al_2O_3 catalysts had more success than any other combination, making up the entire top six catalytic results in terms of DME yield (see Table 1). All other catalysts yielded less than 20% DME. Under this threshold, DME yields observed for different systems are scattered, making it difficult to classify performance based on catalyst type. The CuO–ZnO–ZrO_2 combination was the most utilized catalyst, having the second-best yields (19% DME) after CuO–ZnO–Al_2O_3. HZSM-5 was the most common acidic function catalyst, and its combination with CuO–ZnO–Al_2O_3 was successful overall. Additionally, a majority of the acidic catalysts studied for the one-pot synthesis were zeolites, and therefore, the conversion of CO_2 to DME reaction have not been studied in great detail for other systems (e.g., heteropolyacids).

Concerning the preparation method of the mixed catalysts, physical mixing provided higher DME yields. The co-precipitation method has been employed progressively for hybrid catalyst design, but the highest yield achieved in this method is 36%, leading to the conclusion that further investigation is needed to bring hybrid catalysts into the realm of potential future applications. Overall, the one-pot synthesis of DME for CO_2 holds promise, and a substantial amount of literature has been developed in this regard. Hybrid catalysts in which the active sites are closer in proximity can offer increased preparation efficiency as well as a better yield if prepared correctly, and thus warrant further study. If an optimized catalyst system is prepared, its combination with DAC and other methods of clean CO_2/H_2 production can help us mitigate and find a solution for the greenhouse gas emissions that we are currently battling worldwide.

Acknowledgements We are grateful to Laboratory Directed Research and Development program of Los Alamos National Laboratory for the financial support.

Funding This work was supported by the Laboratory Directed Research and Development program of Los Alamos National Laboratory under Project Grant No. 20220447ER. Los Alamos National Laboratory is operated by Triad National Security, LLC, for the National Nuclear Security Administration of U.S. Department of Energy (Contract No. 89233218CNA000001). FM and MS acknowledge support from the National Science Foundation (grant number 2245474). JM acknowledges funding from Artie McFerrin Department of Chemical Engineering. MS also acknowledges support from TAMU-LANL Development Fellowship awarded by the National Laboratories Office (NLO) of the Texas A&M University System.

Data availability The authors confirm that the data supporting the findings of this study are available within the reference articles and/or its supplementary materials.

Declarations

Conflict of interest The authors report there are no interest conflict to declare.

References

1. Fossil Fuels. Environmental and Energy Study Institute. https://www.eesi.org/topics/fossil-fuels/. Accessed 1 Sept 2023
2. 5 Things you should know about the greenhouse gases warming the planet. United Nations. https://news.un.org/en/story/2022/01/1109322?gclid=CjwKCAjw-IWkBhBTEiwA2exyO1NVIPmYHCoe_SDv51U08X3wF5xMBlXFvrfwPLHhgRaRHqAWNqnv5BoCPUAQAvD_BwE. Accessed 1 Sept 2023
3. Dutta A, Farooq S, Karimi IA, Khan SA (2017) Assessing the potential of CO_2 utilization with an integrated framework for producing power and chemicals. J CO2 Utiliz 19:49–57. https://doi.org/10.1016/j.jcou.2017.03.005
4. Zhu Q (2019) Developments on CO_2-utilization technologies. Clean Energy 3(2):85–100. https://doi.org/10.1093/ce/zkz008
5. Armstrong K, Styring P (2015) Assessing the potential of utilization and storage strategies for post-combustion CO_2 emissions reduction. Front Energy Res 3:8. https://doi.org/10.3389/fenrg.2015.00008
6. Bahruji H, Armstrong RD, Ruiz Esquius J, Jones W, Bowker M, Hutchings GJ (2018) Hydrogenation of CO_2 to dimethyl ether over Brønsted acidic PdZn catalysts. Ind Eng Chem Res 57(20):6821–6829. https://doi.org/10.1021/acs.iecr.8b00230
7. Aresta M, Quaranta E, Tommasi I (1992) Prospects for the utilization of carbon-dioxide. Energy Convers Manage 33(5–8):495–504. https://doi.org/10.1016/0196-8904(92)90048-2
8. Huang CH, Tan CS (2014) A review: CO_2 utilization. Aerosol Air Qual Res 14(2):480–499. https://doi.org/10.4209/aaqr.2013.10.0326
9. Semelsberger TA, Borup RL, Greene HL (2006) Dimethyl ether (DME) as an alternative fuel. J Power Sources 156(2):497–511. https://doi.org/10.1016/j.jpowsour.2005.05.082
10. Asthana S, Samanta C, Bhaumik A, Banerjee B, Voolapalli RK, Saha B (2016) Direct synthesis of dimethyl ether from syngas over Cu-based catalysts: enhanced selectivity in the presence of MgO. J Catal 334:89–101. https://doi.org/10.1016/j.jcat.2015.10.020
11. De Falco M, Capocelli M, Centi G (2016) Dimethyl ether production from CO_2 rich feedstocks in a one-step process: thermodynamic evaluation and reactor simulation. Chem Eng J 294:400–409. https://doi.org/10.1016/j.cej.2016.03.009
12. Guo X, Liu F, Hua Y, Xue H, Yu J, Mao D, Rempel GL, Ng FTT (2023) One-step synthesis of dimethyl ether from biomass-derived syngas on CuO-ZnO-Al_2O_3/HZSM-5 hybrid catalyst: combination method, synergistic effect, water-gas shift reaction and catalytic performance. Catal Today 407:125–134. https://doi.org/10.1016/j.cattod.2022.02.004
13. Xia J, Mao D, Zhang B, Chen Q, Tang Y (2004) One-step synthesis of dimethyl ether from syngas with Fe-modified zeolite ZSM-5 as dehydration catalyst. Catal Lett 98(4):235–240. https://doi.org/10.1007/s10562-004-8686-x
14. Catizzone E, Freda C, Braccio G, Frusteri F, Bonura G (2021) Dimethyl ether as circular hydrogen carrier: catalytic aspects of

hydrogenation/dehydrogenation steps. J Energy Chem 58:55–77. https://doi.org/10.1016/j.jechem.2020.09.040
15. Ghosh S (2016) Production of methanol and DME. https://dst.gov.in/sites/default/files/Survey%20Report%20Production%20of%20Methanol.pdf. Accessed 13 Dec 2023
16. Good DA, Francisco JS, Jain AK, Wuebbles DJ (1998) Lifetimes and global warming potentials for dimethyl ether and for fluorinated ethers: CH_3OCF_3 (E143a), CHF_2OCHF_2 (E134), CHF_2OCF_3 (E125). J Geophys Res Atmos 103(D21):28181–28186. https://doi.org/10.1029/98JD01880
17. Jiang L, Liu W, Wang RQ, Gonzalez-Diaz A, Rojas-Michaga MF, Michailos S, Pourkashanian M, Zhang XJ, Font-Palma C (2023) Sorption direct air capture with CO_2 utilization. Prog Energy Combust Sci 95:101069. https://doi.org/10.1016/j.pecs.2022.101069
18. Yu ZY, Duan Y, Feng XY, Yu X, Gao MR, Yu SH (2021) Clean and affordable hydrogen fuel from alkaline water splitting: past, recent progress, and future prospects. Adv Mater 33(31):e2007100. https://doi.org/10.1002/adma.202007100
19. Marbán G, Valdés-Solís T (2007) Towards the hydrogen economy? Int J Hydrogen Energy 32(12):1625–1637. https://doi.org/10.1016/j.ijhydene.2006.12.017
20. Levin D (2004) Biohydrogen production: prospects and limitations to practical application. Int J Hydrogen Energy 29(2):173–185. https://doi.org/10.1016/s0360-3199(03)00094-6
21. Turner J, Sverdrup G, Mann MK, Maness P-C, Kroposki B, Ghirardi M, Evans RJ, Blake D (2008) Renewable hydrogen production. Int J Energy Res 32(5):379–407. https://doi.org/10.1002/er.1372
22. Holladay JD, Hu J, King DL, Wang Y (2009) An overview of hydrogen production technologies. Catal Today 139(4):244–260. https://doi.org/10.1016/j.cattod.2008.08.039
23. He Y, Liu S, Fu W, Wang C, Mebrahtu C, Sun R, Zeng F (2022) Thermodynamic analysis of CO(2) hydrogenation to higher alcohols (C(2–4)OH): effects of isomers and methane. ACS Omega 7(19):16502–16514. https://doi.org/10.1021/acsomega.2c00502
24. Bansode A, Urakawa A (2014) Towards full one-pass conversion of carbon dioxide to methanol and methanol-derived products. J Catal 309:66–70. https://doi.org/10.1016/j.jcat.2013.09.005
25. Sun K, Lu W, Wang M, Xu X (2004) Low-temperature synthesis of DME from CO_2/H_2 over Pd-modified $CuO–ZnO–Al_2O_3–ZrO_2$/HZSM-5 catalysts. Catal Commun 5(7):367–370. https://doi.org/10.1016/j.catcom.2004.03.012
26. Liaw BJ, Chen YZ (2001) Liquid-phase synthesis of methanol from CO_2/H_2 over ultrafine CuB catalysts. Appl Catal A 206(2):245–256. https://doi.org/10.1016/s0926-860x(00)00601-3
27. Moradi GR, Yaripour F, Vale-Sheyda P (2010) Catalytic dehydration of methanol to dimethyl ether over mordenite catalysts. Fuel Process Technol 91(5):461–468. https://doi.org/10.1016/j.fuproc.2009.12.005
28. Raoof F, Taghizadeh M, Eliassi A, Yaripour F (2008) Effects of temperature and feed composition on catalytic dehydration of methanol to dimethyl ether over γ-alumina. Fuel 87(13–14):2967–2971. https://doi.org/10.1016/j.fuel.2008.03.025
29. Stöcker M (1999) Methanol-to-hydrocarbons: catalytic materials and their behavior. Microporous Mesoporous Mater 29(1–2):3–48. https://doi.org/10.1016/s1387-1811(98)00319-9
30. Rownaghi AA, Rezaei F, Stante M, Hedlund J (2012) Selective dehydration of methanol to dimethyl ether on ZSM-5 nanocrystals. Appl Catal B 119:56–61. https://doi.org/10.1016/j.apcatb.2012.02.017
31. Hu Z-M, Takahashi K, Nakatsuji H (1999) Mechanism of the hydrogenation of CO_2 to methanol on a Cu(100) surface: dipped adcluster model study. Surf Sci 442(1):90–106. https://doi.org/10.1016/s0039-6028(99)00900-0
32. Kattel S, Ramirez PJ, Chen JG, Rodriguez JA, Liu P (2017) Active sites for CO(2) hydrogenation to methanol on Cu/ZnO catalysts. Science 355(6331):1296–1299. https://doi.org/10.1126/science.aal3573
33. Studt F, Behrens M, Kunkes EL, Thomas N, Zander S, Tarasov A, Schumann J, Frei E, Varley JB, Abild-Pedersen F, Norskov JK, Schlogl R (2015) The mechanism of CO and CO_2 hydrogenation to methanol over Cu-based catalysts. ChemCatChem 7(7):1105–1111. https://doi.org/10.1002/cctc.201500123
34. Takeyasu K, Sawaki Y, Imabayashi T, Putra SEM, Halim HH, Quan J, Hamamoto Y, Hamada I, Morikawa Y, Kondo T, Fujitani T, Nakamura J (2022) Hydrogenation of formate species using atomic hydrogen on a Cu(111) model catalyst. J Am Chem Soc 144(27):12158–12166. https://doi.org/10.1021/jacs.2c02797
35. Kattel S, Liu P, Chen JG (2017) Tuning selectivity of CO(2) hydrogenation reactions at the metal/oxide interface. J Am Chem Soc 139(29):9739–9754. https://doi.org/10.1021/jacs.7b05362
36. Zhao Y-F, Yang Y, Mims C, Peden CHF, Li J, Mei D (2011) Insight into methanol synthesis from CO_2 hydrogenation on Cu(111): complex reaction network and the effects of H_2O. J Catal 281(2):199–211. https://doi.org/10.1016/j.jcat.2011.04.012
37. Fujitani T, Nakamura I, Uchijima T, Nakamura J (1997) The kinetics and mechanism of methanol synthesis by hydrogenation of CO_2 over a Zn-deposited Cu(111) surface. Surf Sci 383(2–3):285–298. https://doi.org/10.1016/S0039-6028(97)00192-1
38. Khaleel A, Ma A, Sowaid SB (2019) Ti-doped γ-Al_2O_3 versus ZSM5 zeolites for methanol to dimethyl ether conversion: in-situ DRIFTS investigation of surface interactions and reaction mechanism. Colloids Surf A 571:174–181. https://doi.org/10.1016/j.colsurfa.2019.03.052
39. Kubelkova L, Novakova J, Nedomova K (1990) Reactivity of surface species on zeolites in methanol conversion. J Catal 124(2):441–450. https://doi.org/10.1016/0021-9517(90)90191-L
40. Blaszkowski SR, vanSanten RA (1996) The mechanism of dimethyl ether formation from methanol catalyzed by zeolitic protons. J Am Chem Soc 118(21):5152–5153. https://doi.org/10.1021/ja954323k
41. Naik SP, Ryu T, Bui V, Miller JD, Drinnan NB, Zmierczak W (2011) Synthesis of DME from CO_2/H_2 gas mixture. Chem Eng J 167(1):362–368. https://doi.org/10.1016/j.cej.2010.12.087
42. Ereña J, Garoña R, Arandes JM, Aguayo AT, Bilbao J (2005) Direct synthesis of dimethyl ether from (H_2+CO) and (H_2+CO_2) Feeds. Effect of feed composition. Int J Chem Reactor Eng 3(1). https://doi.org/10.2202/1542-6580.1295
43. Zha F, Tian HF, Yan J, Chang Y (2013) Multi-walled carbon nanotubes as catalyst promoter for dimethyl ether synthesis from CO_2 hydrogenation. Appl Surface Sci 285(2):945–951. https://doi.org/10.1016/j.apsusc.2013.06.150
44. Zha F, Ding J, Chang Y, Ding JF, Wang JY, Ma J (2012) Cu-Zn-Al oxide cores packed by metal-doped amorphous silica-alumina membrane for catalyzing the hydrogenation of carbon dioxide to dimethyl ether. Ind Eng Chem Res 51(1):345–352. https://doi.org/10.1021/ie202090f
45. Bonura G, Frusteri F, Cannilla C, Ferrante GD, Aloise A, Catizzone E, Migliori M, Giordano G (2016) Catalytic features of CuZnZr-zeolite hybrid systems for the direct CO_2-to-DME hydrogenation reaction. Catal Today 277:48–54. https://doi.org/10.1016/j.cattod.2016.02.013
46. Frusteri F, Migliori M, Cannilla C, Frusteri L, Catizzone E, Aloise A, Giordano G, Bonura G (2017) Direct CO_2-to-DME hydrogenation reaction: new evidences of a superior behaviour of FER-based hybrid systems to obtain high DME yield. J CO2 Utiliz 18:353–361. https://doi.org/10.1016/j.jcou.2017.01.030
47. Frusteri F, Bonura G, Cannilla C, Ferrante GD, Aloise A, Catizzone E, Migliori M, Giordano G (2015) Stepwise tuning of

metal-oxide and acid sites of CuZnZr-MFI hybrid catalysts for the direct DME synthesis by CO_2 hydrogenation. Appl Catal B 176:522–531. https://doi.org/10.1016/j.apcatb.2015.04.032
48. Bonura G, Cannilla C, Frusteri L, Mezzapica A, Frusteri F (2017) DME production by CO_2 hydrogenation: key factors affecting the behaviour of CuZnZr/ferrierite catalysts. Catal Today 281:337–344. https://doi.org/10.1016/j.cattod.2016.05.057
49. Ihm S-K, Baek S-W, Park Y-K, Jeon J-K (2003) CO_2 hydrogenation over copper-based hybrid catalysts for the synthesis of oxygenates. In: Ihm SK (ed) Utilization of greenhouse gases, vol 852. ACS symposium series. American Chemical Society, pp 183–194
50. Witoon T, Kidkhunthod P, Chareonpanich M, Limtrakul J (2018) Direct synthesis of dimethyl ether from CO_2 and H_2 over novel bifunctional catalysts containing CuO-ZnO-ZrO_2 catalyst admixed with WOx/ZrO_2 catalysts. Chem Eng J 348:713–722. https://doi.org/10.1016/j.cej.2018.05.057
51. Zhao YQ, Chen JX, Zhang JY (2007) Effects of ZrO_2 on the performance of CuO-ZnO-Al_2O_3/HZSM-5 catalyst for dimethyl ether synthesis from CO_2 hydrogenation. J Nat Gas Chem 16(4):389–392. https://doi.org/10.1016/S1003-9953(08)60009-2
52. Temvuttirojn C, Chuasomboon N, Numpilai T, Faungnawakij K, Chareonpanich M, Limtrakul J, Witoon T (2019) Development of SO_4^{2-}–ZrO_2 acid catalysts admixed with a CuO-ZnO-ZrO_2 catalyst for CO_2 hydrogenation to dimethyl ether. Fuel 241:695–703. https://doi.org/10.1016/j.fuel.2018.12.087
53. Şeker B, Dizaji AK, Balci V, Uzun A (2021) MCM-41-supported tungstophosphoric acid as an acid function for dimethyl ether synthesis from CO_2 hydrogenation. Renewable Energy 171:47–57. https://doi.org/10.1016/j.renene.2021.02.060
54. Schumann J, Eichelbaum M, Lunkenbein T, Thomas N, Álvarez Galván MC, Schlögl R, Behrens M (2015) Promoting strong metal support interaction: doping ZnO for enhanced activity of Cu/ZnO: M (M = Al, Ga, Mg) catalysts. ACS Catal 5(6):3260–3270. https://doi.org/10.1021/acscatal.5b00188
55. Kornas A, Grabowski R, Sliwa M, Samson K, Ruggiero-Mikolajczyk M, Zelazny A (2017) Dimethyl ether synthesis from CO_2 hydrogenation over hybrid catalysts: effects of preparation methods. React Kinet Mech Catal 121(1):317–327. https://doi.org/10.1007/s11144-017-1153-7
56. Ateka A, Sierra I, Erena J, Bilbao J, Aguayo AT (2016) Performance of CuO-ZnO-ZrO_2 and CuO-ZnO-MnO as metallic functions and SAPO-18 as acid function of the catalyst for the synthesis of DME co-feeding CO_2. Fuel Process Technol 152:34–45. https://doi.org/10.1016/j.fuproc.2016.05.041
57. Frusteri F, Cordaro M, Cannilla C, Bonura G (2015) Multifunctionality of Cu-ZnO-ZrO_2/H-ZSM5 catalysts for the one-step CO_2-to-DME hydrogenation reaction. Appl Catal B 162:57–65. https://doi.org/10.1016/j.apcatb.2014.06.035
58. Melián-Cabrera I, Granados ML, Fierro JLG (2002) Pd-modified Cu–Zn catalysts for methanol synthesis from CO_2/H_2 mixtures: catalytic structures and performance. J Catal 210(2):285–294. https://doi.org/10.1006/jcat.2002.3677
59. Pasupulety N, Driss H, Alhamed YA, Alzahrani AA, Daous MA, Petrov L (2015) Influence of preparation method on the catalytic activity of Au/Cu-Zn-Al catalysts for CO_2 hydrogenation to methanol. Proc Bulg Acad Sci 68(12):1511
60. Liu LN, Fan F, Bai MM, Xue F, Ma XR, Jiang Z, Fang T (2019) Mechanistic study of methanol synthesis from CO_2 hydrogenation on Rh-doped Cu(111) surfaces. Mol Catal 466:26–36. https://doi.org/10.1016/j.mcat.2019.01.009
61. Xu J, Su X, Liu X, Pan X, Pei G, Huang Y, Wang X, Zhang T, Geng H (2016) Methanol synthesis from CO_2 and H_2 over Pd/ZnO/Al_2O_3: catalyst structure dependence of methanol selectivity. Appl Catal A 514:51–59. https://doi.org/10.1016/j.apcata.2016.01.006
62. Rui N, Wang ZY, Sun KH, Ye JY, Ge QF, Liu CJ (2017) CO_2 hydrogenation to methanol over Pd/In_2O_3: effects of Pd and oxygen vacancy. Appl Catal B 218:488–497. https://doi.org/10.1016/j.apcatb.2017.06.069
63. Wu CY, Zhang P, Zhang ZF, Zhang LJ, Yang GY, Han BX (2017) Efficient hydrogenation of CO_2 to methanol over supported subnanometer gold catalysts at low temperature. ChemCatChem 9(19):3691–3696. https://doi.org/10.1002/cctc.201700872
64. Lian Y, Fang TF, Zhang YH, Liu B, Li JL (2019) Hydrogenation of CO_2 to alcohol species over Co@Co_3O_4/C-N catalysts. J Catal 379:46–51. https://doi.org/10.1016/j.jcat.2019.09.018
65. Li CS, Melaet G, Ralston WT, An K, Brooks C, Ye Y, Liu YS, Zhu J, Guo J, Alayoglu S, Somorjai GA (2015) High-performance hybrid oxide catalyst of manganese and cobalt for low-pressure methanol synthesis. Nat Commun 6(1):6538. https://doi.org/10.1038/ncomms7538
66. Chen TY, Cao CX, Chen TB, Ding XX, Huang H, Shen L, Cao XY, Zhu MH, Xu J, Gao J, Han YF (2019) Unraveling highly tunable selectivity in CO_2 hydrogenation over bimetallic In-Zr oxide catalysts. ACS Catal 9(9):8785–8797. https://doi.org/10.1021/acscatal.9b01869
67. Akkharaphatthawon N, Chanlek N, Cheng CK, Chareonpanich M, Limtrakul J, Witoon T (2019) Tuning adsorption properties of $Ga_xIn_{2-x}O_3$ catalysts for enhancement of methanol synthesis activity from CO_2 hydrogenation at high reaction temperature. Appl Surf Sci 489:278–286. https://doi.org/10.1016/j.apsusc.2019.05.363
68. Studt F, Sharafutdinov I, Abild-Pedersen F, Elkjaer CF, Hummelshoj JS, Dahl S, Chorkendorff I, Norskov JK (2014) Discovery of a Ni-Ga catalyst for carbon dioxide reduction to methanol. Nat Chem 6(4):320–324. https://doi.org/10.1038/nchem.1873
69. Pustovarenko A, Dikhtiarenko A, Bavykina A, Gevers LEM, Ramirez A, Russkikh A, Telalovic S, Tapia AA, Hazemann JL, Ould-Chikh S, Gascon J (2020) Metal-organic framework-derived synthesis of cobalt indium catalysts for the hydrogenation of CO_2 to methanol. ACS Catal 10(9):5064–5076. https://doi.org/10.1021/acscatal.0c00449
70. Richard AR, Fan M (2018) The effect of lanthanide promoters on NiInAl/SiO_2 catalyst for methanol synthesis. Fuel 222:513–522. https://doi.org/10.1016/j.fuel.2018.02.185
71. Zhang C, Liao PY, Wang H, Sun J, Gao P (2018) Preparation of novel bimetallic CuZn-BTC coordination polymer nanorod for methanol synthesis from CO_2 hydrogenation. Mater Chem Phys 215:211–220. https://doi.org/10.1016/j.matchemphys.2018.05.028
72. Deerattrakul V, Puengampholsrisook P, Limphirat W, Kongkachuichay P (2018) Characterization of supported Cu-Zn/graphene aerogel catalyst for direct CO_2 hydrogenation to methanol: effect of hydrothermal temperature on graphene aerogel synthesis. Catal Today 314:154–163. https://doi.org/10.1016/j.cattod.2017.12.010
73. Rungtaweevoranit B, Baek J, Araujo JR, Archanjo BS, Choi KM, Yaghi OM, Somorjai GA (2016) Copper nanocrystals encapsulated in Zr-based metal-organic frameworks for highly selective CO(2) hydrogenation to methanol. Nano Lett 16(12):7645–7649. https://doi.org/10.1021/acs.nanolett.6b03637
74. Gao WG, Wang H, Wang YH, Guo W, Jia MY (2013) Dimethyl ether synthesis from CO_2 hydrogenation on La-modified CuO-ZnO-Al2O3/HZSM-5 bifunctional catalysts. J Rare Earths 31(5):470–476. https://doi.org/10.1016/S1002-0721(12)60305-6
75. Zhang YJ, Li DB, Zhang Y, Cao Y, Zhang SJ, Wang KJ, Ding F, Wu J (2014) V-modified CuO-ZnO-ZrO_2/HZSM-5 catalyst for efficient direct synthesis of DME from CO_2 hydrogenation. Catal

Commun 55:49–52. https://doi.org/10.1016/j.catcom.2014.05.026
76. Liu R-w, Qin Z-z, Ji H-b, Su T-m (2013) Synthesis of dimethyl ether from CO_2 and H_2 using a Cu–Fe–Zr/HZSM-5 catalyst system. Ind Eng Chem Res 52(47):16648–16655. https://doi.org/10.1021/ie401763g
77. Zhou XH, Su TM, Jiang YX, Qin ZZ, Ji HB, Guo ZH (2016) CuO-Fe_2O_3-CeO_2/HZSM-5 bifunctional catalyst hydrogenated CO_2 for enhanced dimethyl ether synthesis. Chem Eng Sci 153:10–20. https://doi.org/10.1016/j.ces.2016.07.007
78. Zhang M-H, Liu Z-M, Lin G-D, Zhang H-B (2013) Pd/CNT-promoted $CuZrO_2$/HZSM-5 hybrid catalysts for direct synthesis of DME from CO_2/H_2. Appl Catal A 451:28–35. https://doi.org/10.1016/j.apcata.2012.10.038
79. Qi X, Fei J-H, Zheng X-M, Hou Z-Y (2001) DME synthesis from carbon dioxide and hydrogen over Cu-Mo/HZSM-5. Catal Lett 72:121–124
80. Qin ZZ, Zhou XH, Su TM, Jiang YX, Ji HB (2016) Hydrogenation of CO_2 to dimethyl ether on La-, Ce-modified Cu-Fe/HZSM-5 catalysts. Catal Commun 75:78–82. https://doi.org/10.1016/j.catcom.2015.12.010
81. Aboul-Fotouh SMK, Aboul-Gheit NAK, Naghmash MA (2016) Dimethyletherproduction on zeolite catalysts activated by Cl^-, F^- and/or ultrasonication. J Fuel Chem Technol 44(4):428–436. https://doi.org/10.1016/s1872-5813(16)30022-6
82. Schnee J, Eggermont A, Gaigneaux EM (2017) Boron nitride: a support for highly active heteropolyacids in the methanol-to-DME reaction. ACS Catal 7(6):4011–4017. https://doi.org/10.1021/acscatal.7b00808
83. Ladera RM, Ojeda M, Fierro JLG, Rojas S (2015) TiO_2-supported heteropoly acid catalysts for dehydration of methanol to dimethyl ether: relevance of dispersion and support interaction. Catal Sci Technol 5(1):484–491. https://doi.org/10.1039/c4cy00998c
84. Alharbi W, Kozhevnikova EF, Kozhevnikov IV (2015) Dehydration of methanol to dimethyl ether over heteropoly acid catalysts: the relationship between reaction rate and catalyst acid strength. ACS Catal 5(12):7186–7193. https://doi.org/10.1021/acscatal.5b01911
85. Peinado C, Liuzzi D, Ladera-Gallardo RM, Retuerto M, Ojeda M, Pena MA, Rojas S (2020) Effects of support and reaction pressure for the synthesis of dimethyl ether over heteropolyacid catalysts. Sci Rep 10(1):8551. https://doi.org/10.1038/s41598-020-65296-3
86. Millán E, Mota N, Guil-López R, Pawelec B, García Fierro JL, Navarro RM (2020) Direct synthesis of dimethyl ether from syngas on bifunctional hybrid catalysts based on supported H3PW12O40 and Cu-ZnO(Al): effect of heteropolyacid loading on hybrid structure and catalytic activity. Catalysts 10(9):1–22. https://doi.org/10.3390/catal10091071
87. Kornas A, Sliwa M, Ruggiero-Mikolajczyk M, Samson K, Podobinski J, Karcz R, Duraczynska D, Rutkowska-Zbik D, Grabowski R (2020) Direct hydrogenation of CO_2 to dimethyl ether (DME) over hybrid catalysts containing CuO/ZrO_2 as a metallic function and heteropolyacids as an acidic function. React Kinet Mech Catal 130(1):179–194. https://doi.org/10.1007/s11144-020-01778-9
88. Yu YH, Sun DM, Wang SJ, Xiao M, Sun LY, Meng YZ (2019) Heteropolyacid salt catalysts for methanol conversion to hydrocarbons and dimethyl ether: effect of reaction temperature. Catalysts 9(4):320. https://doi.org/10.3390/catal9040320
89. Chen Z, Li XY, Xu YR, Dong YY, Lai WK, Fang WP, Yi XD (2018) Fabrication of nano-sized SAPO-11 crystals with enhanced dehydration of methanol to dimethyl ether. Catal Commun 103:1–4. https://doi.org/10.1016/j.catcom.2017.09.002
90. Sánchez-Contador M, Ateka A, Aguayo AT, Bilbao J (2018) Behavior of SAPO-11 as acid function in the direct synthesis of dimethyl ether from syngas and CO_2. J Ind Eng Chem 63:245–254. https://doi.org/10.1016/j.jiec.2018.02.022
91. Tang Q, Xu H, Zheng YY, Wang JF, Li HS, Zhang J (2012) Catalytic dehydration of methanol to dimethyl ether over micro-mesoporous ZSM-5/MCM-41 composite molecular sieves. Appl Catal A Gen 413:36–42. https://doi.org/10.1016/j.apcata.2011.10.039
92. Witoon T, Permsirivanich T, Kanjanasoontorn N, Akkaraphataworn C, Seubsai A, Faungnawakij K, Warakulwit C, Chareonpanich M, Limtrakul J (2015) Direct synthesis of dimethyl ether from CO_2 hydrogenation over Cu-ZnO-ZrO_2/SO_4^{2-}–ZrO_2 hybrid catalysts: effects of sulfur-to-zirconia ratios. Catal Sci Technol 5(4):2347–2357. https://doi.org/10.1039/c4cy01568a
93. Suwannapichat Y, Numpilai T, Chanlek N, Faungnawakij K, Chareonpanich M, Limtrakul J, Witoon T (2018) Direct synthesis of dimethyl ether from CO_2 hydrogenation over novel hybrid catalysts containing a Cu ZnO ZrO_2 catalyst admixed with WO_x/Al_2O_3 catalysts: effects of pore size of Al_2O_3 support and W loading content. Energy Convers Manage 159:20–29. https://doi.org/10.1016/j.enconman.2018.01.016
94. Ladera R, Finocchio E, Rojas S, Fierro JLG, Ojeda M (2012) Supported niobium catalysts for methanol dehydration to dimethyl ether: FTIR studies of acid properties. Catal Today 192(1):136–143. https://doi.org/10.1016/j.cattod.2012.01.025
95. Dennis-Smither BJ, Yang Z, Buda C, Liu X, Sainty N, Tan X, Sunley GJ (2019) Getting zeolite catalysts to play your tune: methyl carboxylate esters as switchable promoters for methanol dehydration to DME. Chem Commun 55(92):13804–13807. https://doi.org/10.1039/c9cc06334j
96. Rosadi I, Athikaphan P, Chantanachat P, Neramittagapong A, Neramittagapong S (2020) The catalytic activity of Co/kaolinite catalyst for dimethyl ether synthesis via methanol dehydration. Energy Rep 6:469–473. https://doi.org/10.1016/j.egyr.2020.11.212
97. Wang PF, Zha F, Yao L, Chang Y (2018) Synthesis of light olefins from CO_2 hydrogenation over (CuO-ZnO)-kaolin/SAPO-34 molecular sieves. Appl Clay Sci 163:249–256. https://doi.org/10.1016/j.clay.2018.06.038
98. Pranee W, Neramittagapong S, Assawasaengrat P, Neramittagapong A (2016) Methanol dehydration to dimethyl ether over strong-acid-modified diatomite catalysts. Energy Sources A Recov Util Environ Eff 38(21):3109–3115. https://doi.org/10.1080/15567036.2015.1132285
99. Rodriguez-Vega P, Ateka A, Kumakiri I, Vicente H, Ereña J, Aguayo AT, Bilbao J (2021) Experimental implementation of a catalytic membrane reactor for the direct synthesis of DME from H_2+CO/CO_2. Chem Eng Sci 234:116396–116396. https://doi.org/10.1016/j.ces.2020.116396
100. Yang G, Tsubaki N, Shamoto J, Yoneyama Y, Zhang Y (2010) Confinement effect and synergistic function of H-ZSM-5/Cu-ZnO-Al_2O_3 capsule catalyst for one-step controlled synthesis. J Am Chem Soc 132(23):8129–8136. https://doi.org/10.1021/ja101882a
101. Yang GH, Thongkam M, Vitidsant T, Yoneyama Y, Tan YS, Tsubaki N (2011) A double-shell capsule catalyst with core-shell-like structure for one-step exactly controlled synthesis of dimethyl ether from CO_2 containing syngas. Catal Today 171(1):229–235. https://doi.org/10.1016/j.cattod.2011.02.021
102. Nie RF, Lei H, Pan SY, Wang LN, Fei JH, Hou ZY (2012) Core-shell structured CuO-ZnO@H-ZSM-5 catalysts for CO hydrogenation to dimethyl ether. Fuel 96(1):419–425. https://doi.org/10.1016/j.fuel.2011.12.048
103. Phienluphon R, Pinkaew K, Yang GH, Li J, Wei QH, Yoneyama Y, Vitidsant T, Tsubaki N (2015) Designing core (Cu/ZnO/

Al_2O_3)-shell (SAPO-11) zeolite capsule catalyst with a facile physical way for dimethyl ether direct synthesis from syngas. Chem Eng J 270:605–611. https://doi.org/10.1016/j.cej.2015.02.071
104. Tan L, Zhang PP, Suzuki Y, Li HJ, Guo LS, Yoneyama Y, Chen JG, Peng XB, Tsubaki N (2019) Bifunctional capsule catalyst of Al_2O_3@Cu with strengthened dehydration reaction field for direct synthesis of dimethyl ether from syngas. Ind Eng Chem Res 58(51):22905–22911. https://doi.org/10.1021/acs.iecr.9b04864
105. Li F, Ao M, Hung Pham G, Jin Y, Hoang Nguyen M, Majd Alawi N, Tade MO, Liu S (2020) A novel UiO-66 encapsulated 12-silicotungstic acid catalyst for dimethyl ether synthesis from syngas. Catal Today 355:3–9. https://doi.org/10.1016/j.cattod.2019.07.057
106. Kong H, Li HY, Lin GD, Zhang HB (2011) Pd-decorated CNT-promoted Pd-Ga_2O_3 catalyst for hydrogenation of CO_2 to methanol. Catal Lett 141(6):886–894. https://doi.org/10.1007/s10562-011-0584-4
107. Cara C, Secci F, Lai SR, Mameli V, Skrodczky K, Russo PA, Ferrara F, Rombi E, Pinna N, Mureddu M, Cannas C (2022) On the design of mesostructured acidic catalysts for the one-pot dimethyl ether production from CO_2. J CO2 Utiliz 62:102066. https://doi.org/10.1016/j.jcou.2022.102066
108. Ateka A, Pérez-Uriarte P, Gamero M, Ereña J, Aguayo AT, Bilbao J (2017) A comparative thermodynamic study on the CO_2 conversion in the synthesis of methanol and of DME. Energy 120:796–804. https://doi.org/10.1016/j.energy.2016.11.129
109. Sierra I, Ereña J, Aguayo AT, Arandes JM, Bilbao J (2010) Regeneration of CuO-ZnO-Al_2O_3/γ-Al_2O_3 catalyst in the direct synthesis of dimethyl ether. Appl Catal B 94(1–2):108–116. https://doi.org/10.1016/j.apcatb.2009.10.026
110. Wang Y, Wang G, van der Wal LI, Cheng K, Zhang Q, de Jong KP, Wang Y (2021) Visualizing element migration over bifunctional metal-zeolite catalysts and its impact on catalysis. Angew Chem Int Ed Engl 60(32):17735–17743. https://doi.org/10.1002/anie.202107264
111. Tan KB, Xu K, Cai D, Huang J, Zhan G (2023) Rational design of bifunctional catalysts with proper integration manners for CO and CO_2 hydrogenation into value-added products: a review. Chem Eng J 463:142262. https://doi.org/10.1016/j.cej.2023.142262
112. Ma S, Li X, Yang Z, Li H (2023) Size effect of encapsulated metal within zeolite: biomass, CO_2 and methane utilization. J Catal 417:368–378. https://doi.org/10.1016/j.jcat.2022.12.010
113. Arora SS, Shi Z, Bhan A (2019) Mechanistic basis for effects of high-pressure H_2 cofeeds on methanol-to-hydrocarbons catalysis over zeolites. ACS Catal 9(7):6407–6414. https://doi.org/10.1021/acscatal.9b00969
114. Delgado Otalvaro N, Kaiser M, Herrera Delgado K, Wild S, Sauer J, Freund H (2020) Optimization of the direct synthesis of dimethyl ether from CO_2 rich synthesis gas: closing the loop between experimental investigations and model-based reactor design. React Chem Eng 5(5):949–960. https://doi.org/10.1039/d0re00041h

Publisher's Note Springer Nature remains neutral with regard to jurisdictional claims in published maps and institutional affiliations.